STRUCTURE AND EVOLUTION OF LOW MASS STARS

by

Hosein Amiri Khanmakani

A Thesis presented for the Degree of Master of Science in the

University of St Andrews

August 1988.

IN THE NAME OF GOD

To

Jamaran

DECLARATION

I, Hosien Amiri Khanmakani, hereby certify that this thesis has been composed by myself, that it is a record of my own work, and that it has not been accepted in partial or complete fulfilment of any other degree or professional qualification.

Signed ... Date 15/.8./.08.....

UNIVERSITY OF ST. ANDREWS

Thesis Copyright Declaration Form.

A UNRESTRICTED

"In submitting this thesis to the University of St. Andrews I understand that I am giving permission for it to be made available for public use in accordance with the regulations of the University Library for the time being in force, subject to any copyright vested in the work not being affected thereby. I also understand that the title and abstract will be published, and that a copy of the work may be made and supplied to any bona fide library or research worker."

B RESTRICTED

"In submitting this thesis to the University of St. Andrews I wish access to it to be subject to the following conditions:

for a period of years [maximum 5] from the date of submission the thesis shall be

a) withheld from public use.

b) made available for public use only with consent of the head or chairman of the department in which the work was carried out.

I understand, however, that the title and abstract of the thesis will be published during this period of restricted access; and that after the expiry of this period the thesis will be made available for public use in accordance with the regulations of the University Library for the time being in force, subject to any copyright in the work not being affected thereby, and a copy of the work may be made and supplied to any bona fide library or research worker."

Declaration

I wish to exercise option A [i.e. A, Ba or Bb] of the above options.

Signature

Date 15/8/88

CERTIFICATE

This is to certify that H. Amiri Khanmakani has spent seven terms at special studies in the University of St Andrews, that he was admitted under Ordinance No. 51, and that the present thesis embodying the result of his research work can be submitted for the degree of Master of Science.

Signed

Dr T. R. Carson, Supervisor

ACKNOWLEDGEMENTS

I would like to express my thanks to Dr. T. R. Carson, my supervisor, for his valuable advice and guidance which was given throughout the period of my studies, and also for making his opacity data, his code, and other information and data available to me. I also wish to thank Dr. Carson and Professor Stibbs for their very warm welcome on my arrival. Thanks are also due to all staff for their help, and to Mrs Richards for her hospitality in the first year. Finally I am extremely grateful of Ministry of Culture and Higher Education of IRAN for their financial support to continue my studies.

including H^-, H_2, CO, H_2O, CO_2, CN, N_2, and OH. The formula used for energy generation rates are taken from Fowler et al. (1975) in which the screening factor is not considered.

Studies of the input physics parameters are the subject of the Chapter 2. In Chapter 3 we have considered the method of calculating stellar evolution.

Chapter 4 presents our calculated models for both evolutionary intermediate mass and M-S low mass models. A few evolutionary models up to the base of the giant branch are calculated. Section 4-4 represents a set of 18 low mass main sequence models in the mass range $0.1\text{-}1.0 M_\odot$ for both population type compositions. We investigate the effect of molecules on the structure of low mass stars in Section 4-5. We consider the effect of molecular opacities and equation of state as well as the mixing length parameter in low mass stars.

Finally, in the last section, the models are compared with observational data by Reid & Gilmore(1984) and Popper(1980).

Tables Page

Diagrams page

1- INTRODUCTION

1-1 STELLAR STRUCTURE AND EVOLUTION

The aim of stellar structure and evolution is to study the physical laws which determine the stellar variables and the variation of composition inside a star. By an application of these laws to construct theoretical stellar models we can understand the equilibrium configuration in a star, the relation between the basic parameters (e.g. H-R diagram), and the stellar evolution during the time.

What we can observe from stellar properties are energy output, colour, pulsation characteristics, and so on. This subject will describe these properties and show how the observable properties change during the life time of the star and we can also relate these external appearances to the internal structure of the stars.Studies of the stellar interior have been transformed by the application of nuclear physics which provides details of the fundamental physical processes that are responsible for the continual loss of energy at

(1894) introduced the concept of radiative equilibrium which was continued by Schwarzschild and Eddington (2). Eddington also discussed in a series of papers the theory of absorption and emission of radiation within a star in relation to his theory of the hydrostatic equilibrium of a gaseous star (3). The basic mathematical and physical theory of stellar structure and evolution has been investigated by Eddington, Rosseland, Chandrasekhar, Opik, Cowling, Strömgren, Schwarzschild, and Henyey while other authors have supplied an understanding of essential data concerning opacity, degeneracy, thermonuclear processes and element building in star (1).

In recent years (from 1960) Hayashi, Menzel, Cox A. N. , Iben, T. R. Carson and some others have made a great contribution in developing this branch of astrophysics. In relation to his work on stellar opacity T. R. Carson has calculated tables of opacity as a function of temperature and density in different composition. Opacities, including molecular absorption used in low mass models, of this work are those of Carson and Sharp. Tables of these opacities

in the required range of temperature and density for both population I and II compositions are in Section 2-4. We have also used the stellar structure and evolution program using the Henyey method with prescription of Kippenhahn et al. developed by Dr. Carson (TRC/KWH code).

1-2 LOW MASS STARS

In most Galaxies the major fraction of the mass is possibly present in the form of low mass stars as they form, by both number and mass, the largest group of stars in our Galaxy. From a statistical point of view it is important to study this class of star, but they are difficult targets for detailed study and observation because low mass stars are so faint. Many parameters including degeneracy, molecule formation, incomplete ionization, and finally the nonideal gas effects lead to complicated physical and thermodynamical properties, increasingly toward the lower masses. Although the modern instruments and great progress in the theory of stellar structure and evolution have recently enabled astronomers to improve the amount and quality of observation and theoretical

data on the low mass stars, information about these stars, especially very low mass stars, is less available than for the massive stars.

In 1958 Limber(4) used low mass models to study the stars of spectral type M. Hayashi (1962-5)* has shown that low mass models are completely convective and Kumar (1962) has proved that there is a lower limit to the mass of a main-sequence star under which the star becomes completely degenerate or black-dwarf. This type of very low mass star never goes through the normal stellar evolution. Nowadays astronomers use this limit as the transition point in mass between stars and substellar objects. A number of these objects emit radiation for which the wavelength band or colour used to detect them depends on their stage of evolution.These objects are usually referred to as brown dwarfs rather than black dwarfs (see 6).Vardya (1970-7) has worked on the atmosphere, chemical abundances, and source of opacity in late type stars.

*:The second number indicates the reference number.

In recent years great attention has been concentrated on the observational and theoretical work of low and intermediate mass stars. Among other observers, N. Reid has developed the studies of late type stars in a series of papers. In 1984 Reid and Gilmore (8) presented infrared photometry of a large sample of low mass dwarfs. They found that all known low mass dwarfs lie near the expected hydrogen burning main-sequence in the H-R diagram. Our results will be compared with Reid's data as well as that of Popper (1980-33).

A theoretical calculated series of models using a numerical equation of state allowing for particle interactions, as well as H_2O and CO opacities was presented by Grossman et al. (1974-13). Neece (1984-22) adopted opacities including more molecules and also a good equation of state. In 1979 a set of 247 evolutionary sequences were computed by Mengel (see section 4-1) for the mass range $0.55 \leq M/M_{\odot} \leq 6.9$ of which most of the models have masses less than

3.0 $M_{\odot}$. Recent work on the evolutionary models for low and intermediate mass stars has been undertaken by G. Bertelli et al.(1986-9). More recently Liebert and Ronald (1987-6) have compiled a theoretical and observational treatise on the very low mass stars, as well as comparing the two kinds of data.

The most detailed analysis of the low mass main sequence stars has been done by Grossman et al. (13) and Neece (22). Their input physics has resulted in the best agreement with the observation. We have compared our models with their results in the last chapter.

2- STRUCTURE AND EVOLUTION

2-1 PHYSICAL PROPERTIES AND EQUATION OF STATE

To make a stellar model we need to know the composition and local state of the stellar material. Physical processes which determine the evolution of a star depend strongly on the physical state (gas, liquid, or solid) and the abundance of the elements. Normal stars, such as the sun, are so hot that they must be entirely gaseous. The solid and liquid states may arise only under condition of very low temperature and high density. The majority of stars, however, are normal gaseous stars.

The thermodynamical behaviour of gases plays an important part in the studies of stellar structure.The thermal energy of a gas, which is the kinetic energy of moving particles (thermokinetic energy), depends on the temperature of the gas. If the gas is hot the particles move rapidly (energetically) but if it is cool they are

less energetic and the atoms may combine to form molecules.One needs more complicated physical relations to describe the state of the gas at low temperature and relatively high density. Temperature, density, and pressure of the gas are the fundamental quantities in the equilibrium equations of a star. We shall need the equation of state which relates these parameters.

In most stars we can assume that the material is a perfect gas, because the thermodynamical treatment of the non interacting gas is approximately the same as that of the ideal gas, whereas in the dense, relatively cold interiors of the low mass stars the equation of state may involve many non ideal effects. The equation of state of an ideal gas can be put in the form ;

$$P_g(r)=n(r)\ k\ T(r) \qquad (2.1\text{-}1)$$

where r can be distance from the centre of the spherical star. In this equation the gas pressure $P_g(r)$ is related to n(r) the density of free particles and T(r) the gas temperature. In a star total pressure is the sum of gas pressure, P_g, and radiation pressure, P_r. The

number density n(r) depends on the elemental abundances and density of the gas .

When work begun on stellar elemental abundances, helium and hydrogen were considered to be present in such small quantities that they could be ignored. But when the relative strength of the Balmer lines and strong helium lines (in hot stars) were discovered by spectrographic analysis of some stars, it was realized that hydrogen and after that helium are the most abundant elements in stellar atmospheres. They are also the most abundant in stellar interior (in agreement with theoretical studies), because in stellar birth there must not be any process which could cause any considerable difference between the composition of the stellar interior and that of the surface layers. Differences will of course develop since the interior composition changes by the nuclear burning. These days there is no doubt that the most abundant element in the stars is hydrogen, followed by helium, in a manner that one can say the uncertainty in the chemical composition is essentially due to the uncertainty in the abundance of these, the

two lightest elements.

Let X denotes the mass fraction of matter which consists of hydrogen, Y denotes that of helium, and Z the remaining fraction consisting of all heavier elements such that the three fractions fulfil the relation

$$X+Y+Z=1$$

Now we can tabulate the number of atoms and those of corresponding electrons per cubic centimeter as follows (see 10) ;

Elements	Hydrogen	Helium	Heavier
No. of atoms	$X\rho/m_H$	$Y\rho/4\,m_H$	$Z\rho/Am_H$
No. of electrons	$X\rho/m_H$	$2\,Y\rho/4m_H$	$1/2\,AZ\rho/Am_H$

taking into account the fact that in a completely ionized gas all the electrons are free . In this table ρ is the mass density of the matter, m_H is the mass of a hydrogen atom, and A is the average atomic weight for the heavier elements. The first item in the last column is generally negligibly small because the abundance of the heavier

elements, Z, is much less than 1 and A is relatively large. So total number of particles will be

$$n(r) = (2X + 3/4\ Y + 1/2\ \ Z)\ \rho/m_H. \qquad (2.1 - 2)$$

We can use

$$2\,X + 3/4\,Y + 1/2\,Z = 1/\mu$$

in which μ is the mean molecular weight and is used as the composition symbol in stars. For a star of pure atomic hydrogen $\mu=1$ (measured in proton mass), in completely ionized hydrogen gas $\mu=1/2$, and in white dwarfs where hydrogen is negligible $\mu\approx2$. From above we can write n(r) as ;

$$n(r) = \rho/(\mu m_H) \qquad (2.1 -3)$$

and the equation of state (2.1-1) becomes

$$P_{g(r)} = 1/\mu\ k/m_H\ \rho(r)\ T(r)\ . \qquad (2.1 -4)$$

In low density and high temperature stars, where hydrogen and helium are practically completely ionized, and the stellar gases behave thermodynamically as in the ideal gas, this equation will be

justified . The incomplete ionization of the heavier elements is negligible because of their low abundances. But the high density and low temperature of low mass stars requires the use of an equation of state including all the main nonideal gas effects such as; incomplete ionization, molecule formation, electron degeneracy, and Coulomb screening. These effects become more important as the stellar models move to lower mass and the calculation of the equation of state becomes more difficult. As the result of this deviation the properties of stellar configurations near the hydrogen burning mass limit (about 0.08 $M_{\odot}$) are peculiarly uncertain.

In their analysis of the constitutive physics for low mass main sequence models, Grossman et al. (1974-13) have investigated some of these effects. The results of work on a 0.35 $M_{\odot}$ model by Neece (1984-22) showed that neglecting nonideal gas effects will cause a considerable change in the position of the model in the H-R diagram. His results are useful for understanding what change results from varying the input physics (see also 21).

In the case of incomplete ionization, in general, one can write the total pressure in the gas as the sum of partial pressure due to each constituent. Therefore when no molecule formation occurs we may write

$$P_g = P_{atoms} + P_{ions} + P_{electrons}$$

using (2.1 -1) we have

$$P_g = [n_a(r)+n_i(r)+n_e(r)]\, kT.$$

By a simple statistical calculation we can find gas pressure as a function of electron pressure

$$P_g = P(r,\beta_i,X_i)\, P_e \qquad (2.1\text{-}5)$$

in which coefficient P depends on the r, radius, β_i, ionization parameters, and X_i, the elemental abundances. P_e (electron pressure) of course, is

$$P_e = n_e\, k\, T$$

In the case of molecule formation, in general, when two atoms,

A and B, combine to form a molecule we have the reaction

$$A + B \leftrightarrow AB$$

(in particular e. g. $H+H \leftrightarrow H_2$ etc.). We can introduce a dissociation coefficient K_{AB} similar to the Saha's equation of ionization

$$K_{AB} = Z_A Z_B / Z_{AB} \, (2 \pi M_{AB} kT/h^2)^{3/2} \, e^{-D/kT}, \qquad (2.1\text{-}6)$$

defined so that

$$N_A N_B / N_{AB} = K_{AB} \qquad (2.1\text{-}7)$$

in which N_i denote the number densities of the particles. In the equation (2.1-6) D is the molecular dissociation energy and Z_i partition function of the elements. Partition function in this case involves the contribution of the rotation, vibration, and electronic parts(see Carson-2). $\mathfrak{N}_i(=N_i+N_{AB})(i=A,B)$ define the total number of atom i, so we can write the fraction of free atoms as $f_i=N_i/\mathfrak{N}_i$. Using (2.1-7) we have $\mathfrak{N}_i=N_i+N_iN_j/K_{AB}$ (j=B,A) by which we can find the quadratic equation to solve for f_i;

$$\alpha_i f_i^2+(1-\alpha_i+\alpha_j)f_i-1 = 0 \quad (\alpha_i=\mathfrak{N}_i/K_{AB}).$$

f_i will be included in the total number of free particles in the equation of state.

For a degenerate gas the equation of state is a complicated

function of density

$$P_g = P(\rho)$$

where the degeneracy parameter (η) has great role in the function.

The equation of state used in TRC/KWH code includes H, He, C, N, and O with full ionization equilibrium for all stages of ionization. Formation of H^- also is included. Pressure ionization is treated by reducing the ionization potential by an amount equal to the potential at r=0. For a uniform density electron gas enclosed in a sphere of radius R we have

$$V = 3e^2/(2\,R)\,Z^* [1-1/3\,(r/R)^2]$$

where $R=[3/(4\pi N_a)]^{1/3}$ is the radius of the average atomic sphere (N_a = density of atoms /ions) and $Z^* = 4/3\ \pi R^3 N_e$ is the number of free electrons in the sphere (N_e = electron density). Then the decrease in the ionization potential is

$$\Delta I = -3/2\ e^2/R\,Z^*.$$

For the calculation of low mass models formation of H_2 and CO, the

most abundant diatomic molecules, are included by computing the fraction of free atoms (f_i) involved in these molecules.

2-2 ENERGY PRODUCTION SOURCES

2-2.1 STELLAR ENERGY

What energy source supplies the flux which comes through the surface of a star ? The luminosity of most stars does not seem to vary much with time during several billion years, as it is shown by observation of stars during their life-time and geological evidence of the Sun. It indicates that energy must be generated by sources in the stellar interior.

There can be three sources of energy inside a star; thermal energy of stellar gas particles, gravitational energy due to the self gravitational contraction, and nuclear energy through the building up of heavy atoms out of the lightest and most abundant ones, hydrogen and helium. Although in a normal star the energy radiated at the surface is supplied by nuclear reactions, useful information can be obtained by investigation of other sources.

In a gas with temperature T thermal energy of a particle is

$$E_T = 3/2\, kT.$$

If m be the mean molecular weight per particle, then thermal energy of one gram stellar matter is $3/2(k/m)T$ so the thermodynamical energy of the star as a whole is

$$E_T = \int_0^R \frac{3}{2}\frac{kT}{m}\rho 4\pi r^2\, dr \qquad (2.2\text{-}1)$$

where R is the radius of the star.

The gravitational force acting on the internal layers by the outer layers will produce an inward pressure and the resulting gravitational energy per gram of the stellar matter is :

$$E_G = -G\, M_r/r.$$

Where G is the gravitational constant and M_r is the mass of a sphere of radius r which is assumed to be concentrated at the centre of the star. E_G is the required energy to remove one gram of stellar material from infinity to point r. The gravitational energy of the whole star can be written as

$$E_G = \int -G \ M_r/r \ \rho 4\pi r^2 \ dr \qquad (2.2\text{-}2)$$

The potential energy can be transformed into kinetic energy of motion introduced by the dynamical theory of stellar structure and one form of kinetic energy is heat.

The Virial Theorem gives the relation between the thermal energy and the potential energy. From hydrostatic equilibrium (see section 3-1) we have

$$dP/dr = -\rho \ GM_r/r^2. \qquad (2.2\text{-}3)$$

Multiplying by $4\pi r^3$ and integrate over the star

$$dP \ 4\pi r^3 = -\rho \ GM_r/r^2 \ 4\pi r^3 \, dr$$

$$\int dP \ 4\pi r^3 = \int -\rho \ GM_r/r \ 4\pi r^2 \ dr.$$

Using integration by part in the left side we have

$$(P4\pi r^3 \ |_{\text{centre}}^{\text{surface}}) - \int_0^R 3 \ P \ 4\pi r^2 \ dr = \int_0^R -\rho G \frac{M_r}{r} 4\pi r^2 \ dr$$

or

$$\int 3P \ 4\pi r^2 \, dr = \int \rho \ GM_r/r \ 4\pi r^2 \, dr \qquad (2.2\text{-}4)$$

If we define m as mean molecular weight by mass instead of μ by proton mass ($m=\mu m_H$) the equation of state (2.1-3) will take the form of

$$P(r) = k/m\ \rho(r)T(r). \qquad (2.2\text{-}5)$$

Substituting (2.2-5) in the equilibrium equation (2.2-4) we have

$$2\int 3/2\ k/m\ T(r)\rho(r)4\pi r^2\ dr = \int GM_r/r\ \rho(r)4\pi r^2\ dr. \qquad (2.2\text{-}6)$$

The left hand integral is twice the thermal energy and the right hand is directly the negative of gravitational energy ;

$$2E_T = -E_G. \qquad (2.2\text{-}7)$$

This means that only half of the gravitational energy is compensated by thermal energy and the other half will be lost by radiation from the surface. In other words, when a star contracts the self-gravitational force increases so that the internal pressure (and, hence, temperature and heat energy) must also increase to maintain approximate hydrostatic equilibrium. But the gravitational energy decreases (its magnitude increases) twice as fast as the heat energy increases, hence, half of the potential energy change must be radiated into the space.

Nuclear energy generation occurs when a star reaches the main sequence after the pre-main sequence phase. The nuclear processes will take place for the first time when material in the stellar interior reaches a high enough temperature through the contraction process. Nuclear energy is numerically much more than the other two sources, so the main and long-term energy source for stars must be thermonuclear fusion reactions, and the energy loss at the surface as measured by the luminosity is compensated by the energy release from these processes. Since these processes are highly temperature sensitive, raising the central temperature leads to an increase in stellar luminosity which is in agreement with theoretical calculation.

In nuclear processes the light atomic nuclei burn and form heavier nuclei with a slight loss of mass that is converted into energy. This energy corresponds to the binding energy difference between the reacting nuclei and the resulting one, and so depends on the kind of process in which conversion takes place. The most important constituents in reactions are hydrogen and helium because of their high abundance. Since the product of the hydrogen

burning (i.e. helium) becomes nuclear fuel in subsequent reactions, and also because of the relatively long life time of H-burning stage, this reaction is the fundamental nuclear reaction in determining the course of the evolution of the star.

2.2-2 NUCLEAR ENERGY IN LOW MASS STARS

Two different processes contribute in the hydrogen burning stage ; the proton-proton (p-p) chain ,and carbon cycle (C-N). The temperature at the star's centre determines which of the two processes occurs. The p-p reaction is the main energy source in the Sun and in the lower mass (cooler) stars of the main sequence. This direct fusion of hydrogen into helium has three main steps;

$$H^1+H^1\text{-------}> D^2 + e^+ + \upsilon$$

$$D^2+ H^1\text{-------}> He^3+ \gamma \qquad (2.2\text{-}8)$$

$$He^3+He^3\text{--------}> He^4+ 2H^1.$$

Each step also releases some energy and the total amount of energy liberated per helium nucleus formed can be calculated bearing in mind the fact that the first and second reactions have to occur twice, and the energy loss by the neutrinos (υ) must be subtracted.

In addition to these, other possible reactions including $He^3(\alpha,\gamma)Be^7$, $Be^7(p,\alpha)He^4$, $Be^7(e^-,\upsilon)Li^7$, $Li^7(p,\alpha)He^4$, etc may take place. To study the low mass main sequence models some of these reactions also can be taken into account. It depends on the probability of each reaction, the energy release by each step, the existence of each element, and the He^3 abundances. In the lower mass stars it will take a long time for He^3 to accumulate in the star and reach the equilibrium in the $He^3(He^3,2p)He^4$ reaction. Grossman et al. (1974-13) concluded that the He^3 does not reach its equilibrium concentration in a Hubble time for stars of mass less than $0.51M_\Theta$ and F. D'Antona (1985-14) found $0.6M_\Theta$ for this mass limit.

In brown dwarfs ($M<0.08M_\Theta$) the only source of nuclear energy is deuterium burning and the importance of this energy depends on the D^2 abundance (see 14 and 15).Finally in white dwarfs the only source of energy is the thermal energy of the ions.

The C-N cycle, which requires a higher temperature in order to take place, is the main source of energy in massive main sequence

stars. Six reactions contribute to this process to convert four hydrogen nuclei to helium. The products of each step include some energy by which the total energy liberated can be calculated. Although the temperature is very effective in this cycle, it will occur when carbon is available so the population of stars is a parameter. Another important parameter is the probability of each reaction in these two cycles. The reactions have low probability except for a few ones which occur in seconds or minutes. The first step in (2.2-8) takes place in about 14000 million years while the slowest one in C-N cycle take 320 million years. This shows that the p-p interaction is very slow, or the main sequence life time of low mass stars is much longer than that of the massive stars, which is in agreement with numerical calculations (see section 4-3).

The helium burning stage starts when the core becomes hot enough to initiate thermonuclear reaction between the helium nuclei themselves. The ash from the H-burning stage is helium. At the end of the main sequence phase where core hydrogen is exhausted and the shell hydrogen burning (see section 4-1) continues to add mass to the helium core. The core slowly

contracts, there by forcing the star's central temperature to climb. When the central temperature become high enough the reactions will begin to convert helium into heavier elements. Each step of this process produces one heavy element, as well as some energy and the total energy liberated relates to how many reactions take place.

In more massive stars in which the central temperature is higher than that needed for helium burning, or after the exhausion of helium and contraction in the core, other fuel nuclei (e.g. C^{12}, Ne^{20}, and O^{16}) are candidates for burning.

2.2-3 Energy production rate.

The important parameter in the total energy released from the surface of a star is the rate at which nuclear reactions take place. We shall need the energy generation rate ε, which is the energy liberated from nuclear processes per gram of stellar material per second (mean energy production rate is $\bar{\varepsilon}$ =L/M). It is clear that ε depends on the temperature, density, and composition of the star and relates to the rates of the nuclear reaction processes giving the number of reactions, per cubic centimeter per second, which take

place.

The reaction rate also depends on the following parameters :

a) The number of atoms of two kinds (N_1 and N_2) which contribute to the reaction where $N_1 \propto \rho X_1$ and $N_2 \propto \rho X_2$, X_1 and X_2 are the abundances of the two elements.

b) Relative velocity of particles $v(E) = v_1(E_1) - v_2(E_2)$.

c) Cross section of collisions $\sigma(E)$.

d) penetration probability p(E) which relates to the number of collisions.

e) Distribution function $\Psi(E)$ where E can be the kinetic energy of the centre of mass.

We can write the reaction rate as ;

$$r'_{12} = \int N_1 N_2 v(E) \sigma(E) p(E) \Psi(E) dE \qquad (2.2\text{-}9)$$

(see 10,12,and 16).

The reaction rate is sensitive to the Coulomb potential of the nuclei. The potential, especially in low mass and high density regime, is affected by the electron screening and the total potential will be ;

$$V(r) = z_1 z_2 e^2/r + u(r)$$

z_1 and z_2 are atomic charge and r is the distance between the two reacting nuclei. u(r), which is nearly constant, is the screening correction to the Coulomb potential. Since the velocity distribution is in the Maxwellian form this correction enters the reaction rate exponentially. We can write $f_{sc} = e^{-u/kT}$ and the reaction rate will be

$$r_{12} = f_{sc} r'_{12} \qquad (2.2\text{-}10)$$

A general form for the integral (2.2-9) is

$$r'_{12} \propto N_1 N_2 T_6^{-2/3} \exp[-\alpha(z_1^2 z_2^2 A_{1,2}/T_6)^{1/3}] \qquad (2.2\text{-}11)$$

in which $A_{1,2}$ is the reduced atomic mass

$$A_{1,2} = A_1 A_2/(A_1+A_2)$$

and A_i are the atomic masses and α is a constant including π, e, k,and etc.We can write

$$r'_{12} = C\rho^2 X_1 X_2 T_6^{-2/3} \exp[-\alpha(z_1^2 z_2^2 A_{1,2}/T_6)^{1/3}] \qquad (2.2\text{-}12)$$

The energy generation rate is given by, using (2.2-12) in (2.2-10),

$$\varepsilon_{12} = r_{12}\, Q/\rho \quad \text{ergs-g}^{-1}\text{-sec}^{-1}$$

where Q is the total energy release per reaction and $T_6 = T/10^6$ (see 12 and 16).

In our calculation for determination of ε the formula used in the code are taken from Fowler et al.(1975-29)inwhich the screening factor is not included.

2.3 STELLAR ENERGY TRANSPORT

In the last section we found that the energy which escapes from the surface of the star is replaced from the stellar interior, in the case of thermal equilibrium. In this section we will discuss how this energy transports from the stellar centre to the surface.

In a star there exists usually a small departure from temperature, density, and composition balance due to the temperature and density gradients and differences in the chemical composition. This departure gives transport phenomena, among which the energy transport is important. There are three principal mechanisms by which the energy is transported; conduction, convection, and radiation. The total energy flux may be written as;

$$F = F_{cond} + F_{conv} + F_{rad}. \qquad (2.3\text{-}1)$$

Conduction is the basic mode of energy transfer at high density in which energy can be carried by the motion of the degenerate electrons ,although these electrons may be scattered by the ions or other electrons. The flux in this case is defined by;

$$F_{cond} = -K_{cond}\,[dT/dr] \qquad (2.3\text{-}2)$$

where r is measured in the direction of transport. K_{cond} is the thermal conductivity which is suggested by T. R. Carson(1976-17) as;

$$K_{cond} = (2m^3/h^3)[I(1)I(E^2)-I^2(E)]/T\,I(1) \qquad (2.3\text{-}3)$$

where

$$I(x) = 4\pi/3\int x\tau v^4\,\partial f(E)/\partial E\,dv.$$

In this integral $\tau^{-1} = N_s v \sigma_s$ in which N_s and v are the number density and velocity of the scatterer and σ_s is the total scattering cross-section and

$$f(E) = [\exp(E/kT+\eta)+1]^{-1}$$

is the energy distribution function where η is the degeneracy parameter. Thermal conductivity can be obtained by the theory of

metals as ;

$$K_{cond} = (S_{11}S_{12} - S_{12}S_{21})/T\,S_{11} \qquad (2.3\text{-}4)$$

in which S_{ij} are the usual transport coefficients for the particle and thermal currents in the gas. However, conditions inside the star are not favorable for conduction so K_{cond} is very small in normal stars. Energy inside the main sequence stars moves from centre to the surface by two other ways: convection and radiative diffusion.

Convection is the fluid motion between hot and cool regions in which hot gases of the stellar interior rise toward the stellar surface and cool gases of the surface sink down toward the centre. If a fluid element suffers a small displacement, dr, over which the ambient temperature changes by dT and the pressure by dP the change in its temperature is given by the adiabatic law (see 10 & 2)

$$(dT/dr)_{ad} = (1-1/\gamma)T/P\ dP/dr \qquad (2.3\text{-}5)$$

in which $\gamma = C_p/C_v$ where C_p and C_v are the specific heats at constant pressure and constant volume. The necessary condition for convection to take place is that the magnitude of ambient

temperature gradient dT/dr be greater than of the adiabatic temperature gradient.In the other words

$$\Delta \nabla T = |dT/dr| - |dT/dr|_{ad} > 0$$

where the symbol $\Delta \nabla T$ is defined by

$$\Delta \nabla T = (1-1/\gamma)T/P\ dP/dr - dT/dr \qquad (2.3\text{-}6)$$

and denotes the super adiabatic temperature gradient.

We may describe the convective energy transport by the mixing length theory. Each element travels the distance l before mixing with the ambient matter. In the other words l, which is called mixing length, is the mean free path of the convective element and is given by

$$l = \alpha H_p. \qquad (2.3\text{-}7)$$

H_p is the pressure scale height and is defined by

$$1/H_p = 1/P\ |dP/dr| = GM\rho/(Pr^2) \qquad (2.3\text{-}8)$$

(see 16) and α is free parameter which in general is preferred to be 1.0-2.0 especially for intermediate mass stars (see e. g. 9).Cox et al. (1981-32) suggested that α must be much smaller than 1.0 for stars

of $M \leq 0.3 M_{\odot}$ (see also section 4-5). The temperature excess between two points of energy transfer is

$$dT/dr = (1-1/\gamma)T/P\ dP/dr - dT/dr \qquad (2.3\text{-}9)$$

or we can write $\Delta T = \Delta\ \nabla T\ l$. The transferred heat per unit of mass is given by

$$\Delta Q = C_p \Delta T \qquad (2.3\text{-}10)$$

$$= C_p\, l\, \Delta\, \nabla T.$$

So the average excess flux is

$$F_{conv} = \rho v\, \Delta Q \qquad (2.3\text{-}11)$$

or $$F_{conv} = \rho v C_p l\ \Delta\ \nabla T$$

where v is the average velocity of the element and ρ is its density. By a simple calculation we can write

$$F_{conv} = 1/4\ C_p\ \rho (g/T)^{1/2} (\Delta\ \nabla T)^{3/2}\ l^2 \qquad (2.3\text{-}12)$$

which g is surface gravity in a star.Convection is the most efficient case of energy transfer in the low mass stars, although in very low mass stars it is complicated by the degeneracy conduction.

In the TRC/KWH code the convection is treated in the same way

as Kippenhahn et al. (1967-18)in which the standard local mixing-lengh theory of Bohm-Vitense (see 18 for refrence) is used for non-adiabatic convection. The cubic equation given by Kippenhahn et al. is solved for ∇.

The transport of energy by radiation is the principal mode of energy transfer in the nondegenerate regime in which energy is carried by photons. The velocity and path length of the photons will be limited by the interaction of the photons and the matter (absorption and scattering). If the mean free path of the photons be λ and one supposes that at each point the matter emits and absorbs like a black body then the net radiative energy flux between the points of emission and absorption of photon will be

$$F_{rad} = -\Delta(\sigma T^4) \qquad (2.3\text{-}13)$$

$$= -4\sigma T^3 \Delta T$$

(see 2)we know that

$$\sigma = ac/4$$

in which a is the radiation constant and c is the velocity of light. We have now

$$F_{rad} = -ac\lambda T^3 \, dT/dr$$

if we substitute $\Delta T = \lambda \, dT/dr$ in (2.3-13). If $\underline{k}$ be the absorption coefficient per unit of mass we have

$$\lambda = 1/(\rho \underline{k})$$

$$F_{rad} = -ac/(\rho \underline{k}) T^3 \, dT/dr \qquad (2.3\text{-}14)$$

$$= -K_{rad} \, dT/dr$$

where

$$K_{rad} = ac/(\rho \underline{k}) T^3 \qquad (2.3\text{-}15)$$

is radiative conductivity.

The processes which affect the limitation of propagation of the radiation (radiative opacity) are the subject of the next section.

2.4 OPACITY

The radiation photons propagate in the star through a medium which absorbs, emits, and scatters radiation. There are a number of processes that impede the free motion of a photon in the stellar material in which the radiation is weakened by its interaction with the particles. The possible physical processes depend on the state

of the matter which may be in different stage of ionization of the atoms, degenerate electron gas, molecular gas, and even solid, and of course this state in turn depends on the temperature of the matter. Therefore the following processes may contribute to the stellar opacity;

a) Free-free absorption or inverse bremsstrahlung process which in the case of complete ionization (high temperature) a photon will be absorbed by a free electron when it makes a transition to another continum state of higher energy.

b) Scattering: Compton or Thomson scattering of photons by free electrons, Rayleigh scattering of photons by the bound electrons in atoms and molecules in late type stars.

c) Photoexcitation or bound-bound transitions in which an atom absorbs a photon and a bound electron makes a transition to bound state of higher energy.

d) Photoionization or bound -free transitions in which an atom will absorb a photon and a bound electron makes a transition to a continum state. The dissociation of molecules and grains in low

mass stars are other sources of opacity.

The cases of a, c, and d are true-absorption processes, whereas in the case b the photon is not destroyed and will reappear in a new direction with possibly a slightly altered frequency. However, in calculation of opacity all of (or a number of) these processes may be taken into account and the absorption coefficient added together, as the radiative transport equation includes all three parts of emission, absorption, and scattering terms.

The interaction cross-section of the processes and other relevant data, such as energy levels and occupation numbers, needed for opacity calculations are correctly given only by quantum mechanical calculation. We need also the composition of the material (X,Y,Z) and the electron density for which a statistical calculation can be useful (see Carson 2 and 17). If $\sigma_a(\upsilon)$ denotes the cross-section of interactions in which absorption occurs and $\sigma_s(\upsilon)$ that of the scattering then the mass absorption and mass scattering coefficients are given by

$$k_a(\upsilon) = 1/\rho \, N_a \sigma_a(\upsilon) \qquad (2.4\text{-}1)$$

$$k_s(\upsilon) = 1/\rho\, N_s \sigma_s(\upsilon) \qquad (2.4\text{-}2)$$

in which the N_i are the number densities of absorbers or scatterers.

It is possible that only one part of absorbed radiation energy converts to kinetic energy of particles and the other part is re-emitted due to the inverse of the process, stimulated emission. So the absorption coefficient $k_a(\upsilon)$ needs a correction for emission which was first introduced by Rosseland in 1930. We can write the corrected coefficient as

$$k'_a(\upsilon) = k_a(\upsilon)\ (\ 1\text{-}e^{-h\upsilon/kT}\ ) \qquad (2.4\text{-}3)$$

(see 2) in which $1\text{-}e^{-h\upsilon/kT}$ is the correction factor.A correction may also affect the scattering coefficient. Let $p(\omega,\omega')$ be the phase function of scattering from direction ω to ω' with separated angle of ϑ.We may introduce a correction term for scattering into the beam by using the average of the cosine of the scattering angle which is

$$\mu = \int p(\omega,\omega')\, \mathrm{Cos}(\vartheta)\, d\omega' \qquad (2.4\text{-}4)$$

the corrected mass scattering coefficient will be

$$k'_s(\upsilon) = k_s(\upsilon)(1-\mu) \qquad (2.4\text{-}5)$$

The effective absorption coefficient is the sum of these two coefficients

$$k_e(\upsilon) = k'_a(\upsilon)+k'_s(\upsilon) \qquad (2.4\text{-}6)$$

Its application in the equation of transfer is

$$dI/ds = -\rho k_e(\upsilon)I(\upsilon) + \rho J_e(\upsilon) \qquad (2.4\text{-}7)$$

in which $J_e(\upsilon)$ represents the source function.

We can now write the average absorption coefficient of Rosseland:

$$1/k = 1/[dB(T)/dT]\int 1/k_e(\upsilon)\, dB(\upsilon,T)/dT\, d\upsilon \qquad (2.4\text{-}8)$$

in which k is Rosseland mean absorption coefficient or Rosseland mean opacity. $B(\upsilon,T)$ and $B(T)$ are the monochromatic and total radiation function (planck function) such that

$$B(T) = \int B(\upsilon,T)\, d\upsilon \qquad (2.4\text{-}9)$$

and

$$B(\upsilon,T) = (2h\upsilon^3/c^2)/(e^{h\upsilon/kT}-1) \qquad (2.4\text{-}10)$$

Substituting $dB(\upsilon,T)/dT$ from (2.4-10) and (2.4-9) in (2.4-8) we can

find

$$1/k = 15/(4\pi^4) \int u^4 e^u/[k_e(u)(e^u-1)^2]\, du \qquad (2.4\text{-}11)$$

($u=h\upsilon/kT$) giving another form of the mean opacity relation. This (Rosseland) mean opacity can be used for what we introduced in the radiative conductivity (2.3-15).

We may use mass absorption and scattering coefficients in (2.4-11) individually to find opacity in each case. The scattering opacity is independent of both temperature and density and only depends on the composition as it was shown by T. R. Carson(2);

$$k_s = 0.200388(1+X). \qquad (2.4\text{-}12)$$

The absorption opacity, however, will take the form

$$k = k_1 \rho T^{-7/2} \qquad (2.4\text{-}13)$$

which is known as the Kramer's opacity where k_1 depends on the composition. Therefore the total opacity of the stellar gas depends strongly on both the composition of the gas and its thermodynamic stage. One can write for each composition

$$k = k(\rho, T)$$

(see table 2.1 and 2.2).

Finally, thermal conduction of energy transport also may introduce an opacity (see Carson 17) which contributes to the total opacity as

$$1/k_t = 1/k_r + 1/k_c.$$

k_r is the Rosseland mean radiative opacity and k_c, the conductive opacity, can be defined by similar relation as it was for radiative opacity introduced in (2.3-15).

2.4-1 OPACITY IN LOW MASS STARS

In low mass stars where the temperature is not high enough for ionization, most atoms are neutral (especially in the outer layers where they may combine to form molecules) and in addition to atomic processes other sources including molecules and negative ions contribute to the opacity.

In the case of negative ions some of the free electrons (from easily ionized atoms) attach themselves to the neutral atoms. The system consisting of a neutral atom and an electron, in a free or bound state, can interact with the radiation photon via both bound-free and free-free transitions. This process will give rise to the usual free-free or bound-free absorption. The most important

negative ion in the atmospheres of solar type and cooler stars is H^-. Other negative ions or molecules which may contribute to the opacity are H_2^-, He^-, C^-, Cl^-, F^-, H_2O^-, etc(see Vardya 7). According to their stability and abundances either both of these transitions or one of them may be taken into account. Bound-free absorption of H_2^- is not important because of instability of this molecule, while on the other hand, in carbon stars with surface temperature greater than 2500 °K bound-free absorption of C^- provide 10 percent of the opacity (see 7).

Atomic lines, especially H and C, and possibly Thomson scattering may contribute a few percent to the total opacity in cool stars, but photodissociation of molecules and Rayleigh scattering by atoms and molecules are important sources of opacity. As one goes toward lower mass the abundance of molecules will be higher and the bound-bound absorption by pure rotation, vibration rotation, and electronic transition of the molecules become considerable. Normally H_2 is the most important, but in hydrogen deficient composition C_2 and N_2 become major contributors (see 17). Among

the other molecules H_2O is more important than others including TiO, CO, CN, CO_2, etc., of which CO is usually most abundant because of its high binding energy (11.09ev).Other sources of molecular opacity are collision induced absorption by H_2 and bound-free transitions in OH and CH, and the extinction due to the grains in $\log T_e<3.2$ (see 14) can be a source.

We have used Carson and Sharp opacities (1988-in preparation for publication) in our work in which H^-, H_2, CO and other diatomic and triatomic molecules including H_2O, CO_2, CN, N_2, OH are taken into account. We have tabulated these opacities for $\log T_e$=4.0 to 3.3 and $\log\rho$ from -13 to -2 for two compositions in tables 2-1 and 2-2. For $\log T_e>4.0$ the opacity is given by the Christy analytical fit to opacity tables.

Table 2-1:Carson and Sharp opacities including continuous and molecular (diatomic and triatomic) absorption. Entries are log of (Rosseland) opacity in population II (0.783,0.216,0.001) stars.

Log$\rho\downarrow$	←——————————Opacity——————————→							
Log$T_e\rightarrow$	4.0	3.9	3.8	3.7	3.6	3.5	3.4	3.3
-2	3.9209	3.232	2.3112	1.2624	0.5751	-0.0717	-0.7485	-1.4013
-3	3.2184	2.5611	1.6911	0.9549	0.3780	-0.4234	-1.1178	-1.9004
-4	2.5758	1.9000	1.0795	0.3422	-0.3087	-1.1789	-1.8271	-2.7096
-5	2.1196	1.3543	0.5074	-0.3780	-1.0908	-1.8644	-2.7050	-3.5337
-6	1.8054	0.9122	-0.0214	-1.0430	-1.6385	-2.2360	-2.9554	-3.7394
-7	1.5914	0.5533	-0.4964	-1.6411	-2.3370	-2.7646	-3.1433	-3.8305
-8	1.4151	0.2624	-0.9275	-2.1603	-3.0787	-3.6263	-3.2699	-3.8692
-9	1.1401	0.0560	-1.3078	-2.6130	-3.8357	-4.2923	-3.6791	-3.7936
-10	0.5763	-0.0718	-1.5372	-2.9319	-4.2959	-4.6893	-4.7145	-3.8427
-11	-0.0747	-0.1893	-1.4535	-2.9310	-4.3339	-4.8687	-5.3196	-3.9222
-12	-0.4098	-0.3616	-1.1481	-2.6105	-4.1155	-4.9350	-5.382	-4.5023
-13	-0.4903	-0.4784	-0.8129	-2.1744	-3.7915	-4.9629	-5.2816	-5.5111

Table 2-2: Same as Table 2-1 but for population I (0.770, 0.212, 0.018) stars.

Logρ ↓	←----------Opacity----------→							
$LogT_e$→	4.0	3.9	3.8	3.7	3.6	3.5	3.4	3.3
-2	3.9228	3.2723	2.5546	1.9923	1.3762	0.6858	-0.0834	-0.8055
-3	3.2357	2.7104	2.2759	1.8725	1.1699	0.4314	-0.4012	-1.2470
-4	2.574	1.9583	1.5691	1.282	0.5125	-0.2212	-1.0334	-1.8675
-5	2.1133	1.3712	0.7772	0.4738	-0.2242	-0.8911	-1.8235	-2.8333
-6	1.7978	0.9113	0.1006	-0.2423	-0.8064	-1.1834	-2.0198	-3.0539
-7	1.5833	0.5472	-0.4555	-1.0433	-1.4285	-1.6976	-2.0431	-3.1488
-8	1.4066	0.2546	-0.9178	-1.8514	-2.0753	-2.662	-2.3034	-3.1696
-9	1.1301	0.0480	-1.3086	-2.4839	-2.7849	-3.5048	-2.7508	-3.2879
-10	0.5643	-0.0796	-1.5419	-2.8785	-3.4875	-3.9506	-3.8230	-3.3359
-11	-0.0851	-0.1974	-1.4578	-2.9162	-3.9117	-4.1145	-4.7283	-3.4351
-12	-0.4179	-0.3697	-1.1522	-2.6046	-3.9266	-4.1404	-4.8717	-3.8143
-13	-0.4972	-0.4856	-0.8175	-2.1740	-3.6982	-4.1706	-4.7305	-4.8519

2-5: H-R DIAGRAMS

The Hertzsprung-Russell diagram plots the luminosities of stars versus effective surface temperature. The graph also has been plotted as magnitudes of the stars versus color index or spectral type. This graph is a powerful tool which helps us to develop our understanding of stellar evolution.The most convenient form for evolutionary analyses is a plot of $\log L/L_{\Theta}$ versus $\log T_e$,the theoretical H-R diagram.

The position of a star in the H-R diagram is very important as it indicates many factors (such as age, evolutionary phase, spectral type, etc.) and at a given chemical composition will be determined by their masses. According to their positions stars are classified into 3 main groups (see figure 2.1); main sequence, giants, and dwarfs.

The Main Sequence is the location of the chemical homogeneous and thermal equilibrium stars, extended from the hot and bright in the upper-left corner to the cool and dim in the lower-right corner of the diagram. The low mass stars of the lower end of the M-S are often referred to as red dwarfs. M-S stars may be divided into two main groups; Population I and Population II. Population I stars represent young and metal rich and Population II those of old

and metal poor stars. We have worked on populations with Z=0.018, 0.02 and Z=0.001. Figure 2.1 shows a typical H-R diagram (M_v versus B-V) in which visual magnitude can be related to the $\log L/L_\Theta$ by

$$M_v = 4.83-2.5\log L/L_\Theta - B.C.$$

B.C. (bolometric correction) and B-V (color index) are known function of effective temperature.

Figure 2-1:A typical H-R diagram, visual magnitude versus color index which is temperature indicator. The graph is from Hayashi (taken from 12).

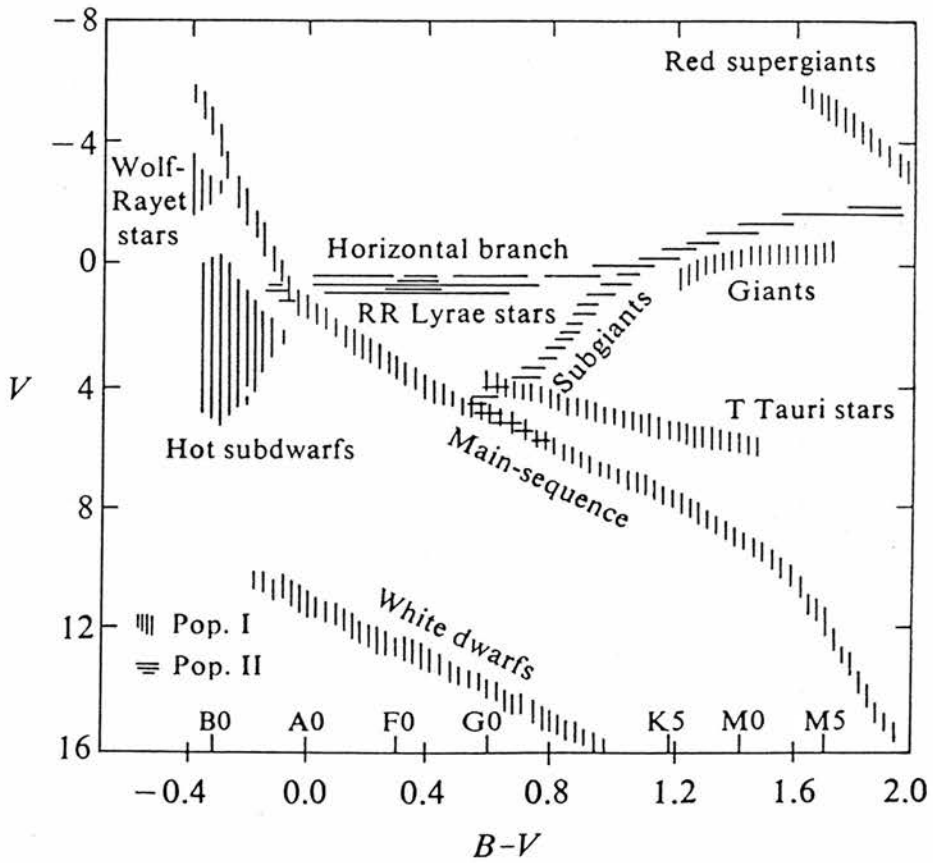

3- STELLAR EVOLUTION CALCULATIONS

3-1 BASIC EQUATIONS

In the last chapter we introduced the basic physical parameters that are used to define a stellar model. In order to determine these parameters we may unify them in a system of equations by using the conservation and equilibrium configurations. The problem will be simplified by assuming spherical symmetry as this will exclude magnetic forces and rotation and therefore reduces the problem to one dimension.

From the mass distribution in the star we have

$$dM_r = 4\pi r^2 \rho \, dr$$

where the corresponding differential equation is

$$dM_r/dr = 4\pi r^2 \rho. \qquad (3.1\text{-}1)$$

Integrating this equation gives the mass within a sphere of radius r around the stellar centre

$$M_r = \int_0^r 4\pi r^2 \rho \, dr \quad .$$

Hydrostatic equilibrium will cause the compensation of gravitational (inward) and pressure gradient (outward) force. The gravitational force acting on the mass element $dM = \rho dv$ is

$$-GM_r/r^2\ \rho dv$$

and the hydrostatic force acting on the volume element dv = dA dr is

$$dP\ dv/dr.$$

The equation of hydrostatic equilibrium then is

$$dP/dr = -\rho GM_r/r^2. \qquad (3.1\text{-}2)$$

In the case of unequilibrium the force due to the acceleration, d^2r/dt^2, will balance the difference between these two forces.

From the conservation of thermal energy we can write

$$\frac{d}{dt}\left(\frac{3}{2}\frac{kT}{m}\right) = -P\frac{dv}{dt} + \varepsilon - \frac{1}{4\pi r^2\rho}\frac{dL_r}{dr}$$

in which the internal energy of one gram of ideal gas per unit of time is balanced by the sum of work done by the pressure P on the specific volume $v(=1/\rho)$, energy gain by nuclear reactions, and energy loss (per second per unit of mass) by luminosity which leaves the surface of radius r. Using equation of state (2.1-3)

$$P = k/m\ \rho T$$

and entropy in the form

$$s = A\log_e(P\rho^{-5/3})+B$$

(A and B are constants) then the energy conservation equation can be written as

$$dL_r/dr = 4\pi r^2 \rho(\varepsilon - Tds/dt). \qquad (3.1\text{-}3)$$

In the case of radiative equilibrium, the temperature gradient is related to the luminosity via the transport equation (2.3-14) by

$$dT/dr = -3/(4ac)\, k\rho/T^3\, L/(4\pi r^2) \qquad (3.1\text{-}4)$$

in which k is opacity. The transport mechanism introduces a mean temperature gradient ∇ which in the radiation and conduction cases (18) can be written as

$$\nabla = 3/(16\pi acG)\, kL_r P/(M_r T^4)$$

from which equation (3.1-4) will be

$$dT/dr = -\rho G M_r/(r^2 P)\, T\, \nabla \qquad (3.1\text{-}5)$$

Equations (3.1-1), (3.1-2), (3.1-3), and (3.1-4) or (3.1-5) are the basic differential equations that involve both space (structure) and time (evolution) which govern the stellar structure and evolution. The solution of these equations then consists of specifying the values of P(r), L(r), T(r), and M(r). Other parameters including ρ, ε, k, s, and ∇ which appear in these equations describe the properties of the stellar material, where ε is the rate of energy production of all nuclear reactions

$$\varepsilon = \sum_k \varepsilon_k$$

The density ρ is the function of pressure, temperature, and composition only. Other parameters can also be defined depending on the same variables

$$\rho = \rho(P, T, X_i)$$

$$k = k(P, T, X_i)$$

$$s = s(P, T, X_i)$$

$$\nabla = \nabla(P, T, X_i) \qquad (3.1\text{-}6)$$

$$\varepsilon = \varepsilon(P, T, X_i)$$

Thus, in order to solve the equations we also need $X_i(=X,Y,Z)$.

The composition change of ith element can be defined as

$$X_i(t+\Delta t, r) = X_i(t, r)+(\partial X_i/\partial t)_{\text{nuc. reac.}}\, \Delta t \qquad (3.1\text{-}7)$$

where $X_i(0, r)$ are the initial abundances. The two important mechanisms by which the composition changes are nuclear reactions and mixing by convection. In a convection zone the chemical composition is homogeneous because of the short time of mixing material relative to the time scales of stellar evolution phases. If we ignore the mixing from the boundaries of the two sides of the zone, then the only mechanism is that due to nuclear reactions by which some nuclei are destroyed and some

synthesized. We can write

$$\frac{\partial X_i}{\partial t} = -\sum_{k'} \frac{\varepsilon_{k'}}{Q_{ik'}} + \sum_{k''} \frac{\varepsilon_{k''}}{Q_{ik''}} \qquad (3.1\text{-}8)$$

in which $Q_{ik'}$ is the energy gained (per gram) when element i is destroyed and $Q_{ik''}$ is the energy gained when it is produced.

The range of the independent variable r is unspecified. It might be more convenient to choose a lagrangian variable in place of the radius. We usually prefer to study a model of a star of mass M rather than a star of radius R. If M_r is the mass of a sphere of radius r around the centre, then the corresponding r will be obtained by solving for the function r(M) in (3.1-1). All unknown functions also can be considered dependent only upon M_r, and the time t. The problem of the stellar evolution is then the determination of the functions

$$\begin{aligned} r &= r(M_r, t) \\ P &= P(M_r, t) \\ L &= L(M_r, t) \\ T &= T(M_r, t) \end{aligned} \qquad (3.1\text{-}9)$$

$$X_i = X_i(M_r, t).$$

We can now change the equations (3.1-1), (3.1-2), (3.1-3), (3.1-5), and (3.1-7) to

$$dr/dM_r = 1/(4\pi r^2\rho) \qquad (3.1\text{-}10)$$

$$dP/dM_r = -GM_r/(4\pi r^4) \qquad (3.1\text{-}11)$$

$$dL/dM_r = \varepsilon - Tds/dt \qquad (3.1\text{-}12)$$

$$dT/dM_r = -GM_rT/(4\pi r^4P)\ \nabla \qquad (3.1\text{-}13)$$

$$X_i(t+\Delta t, M) = X_i(t, M)+dX_i/dt\ \Delta t. \qquad (3.1\text{-}14)$$

The equations (3.1-10) through (3.1-14) gives us as many equations as there are unknown variables, namely r, P, L, T, and X_i.

At a given composition all the functions and parameters will be defined by the mass of the star through the equations (3.1-9) and (3.1-6). Therefore the structure of a star is uniquely determined by its mass and chemical composition. In stellar evolution X_i may be used as initial composition and their local values at any time t will be determine by equations (3.1-14) and (3.1-8).

If convection dominates the energy transport, as in low mass stars, then the equation of adiabatic temperature gradient (2.3-5) will be used in place of temperature gradient (3.1-4) to find

$$dT/dM = (1-1/\gamma)\, T/P\, dP/dM. \qquad (3.1\text{-}15)$$

We can now replace equation (3.1-13) by (3.1-15). The rate of energy generation will also be affected by the convection partly due to the composition change. Iben and Renzini (1983-19) have detailed the effect of the mixing process on the composition of the low mass stars.

3.2 BOUNDARY CONDITIONS

The initial conditions for the solution of the first order non-linear differential equations (3.1-10) to (3.1-13) are boundary conditions.These conditions are the satisfaction of the variables at the surface and the centre of the star by the equations. The equations, however, must all be fulfilled in every layer of the star including the surface layer with

$$M_r = M, \qquad T = T_{eff}(L, R) \quad \text{and } r = R \qquad (3.2\text{-}1)$$

and the centre with

$$M_r = 0, \quad L_r = r = 0 \quad \text{and } p, T, \rho = (P_c, T_c, \rho_c) \qquad (3.2\text{-}2)$$

M, L, and R denote the total mass, luminosity, and radius of the star where T_{eff} is the effective surface temperature.We shall need the behaviour of T, r, L, and P (regular solutions) at each boundary

level.

For a model of mass M and given composition the values of R and L are observable, and so can be assumed, from which one can determine the temperature by the black body relation

$$T_{eff}^4 = L/(4\pi\sigma R^2). \qquad (3.2\text{-}3)$$

We also need a surface boundary conditions for the pressure which may be obtained from the atmospheric equations.

In the atmosphere of the star (lower temperature region) temperature is sensitive to the opacity or optical depth τ defined by

$$d\tau = -k\rho dr \qquad (3.2\text{-}4)$$

where $\tau(r=0) = 0$ and k is the opacity. In fact above the layer r = R and $T=T_{eff}$ in which the energy is transported efficiently by radiation, the radiative temperature gradient (3.1-4) drops as the density decreases. Thus there is not a considerable change in the temperature with the mass above this layer but it depends on the optical depth and may be defined by a general form

$$T = T(L, R, \tau). \qquad (3.2\text{-}5)$$

The layer r = R and $T = T_{eff}$ is a photosphere (the bottom of the atmosphere) at the optical depth

$$\tau = \int_{r_{ph}=R}^{\infty} k\rho \, dr$$

$$= 2/3$$

from which photons can escape. Therefore, one can obtain T_{eff} by substituting τ in the atmospheric equation (3.2-5)

$$T_{eff} = T(L, R, \tau)$$

$$= [L/(4\pi\sigma R^2)]^{1/4} \qquad (3.2\text{-}6)$$

Equations (3.1-10) and (3.2-4) may combine to form

$$dM_r/d\tau = dM_r/dr \; dr/d\tau$$

$$= -4\pi R^2/k.$$

We have

$$dP/d\tau = dP/dM \; dM/d\tau$$

which using (3.1-11) we will find

$$dP/d\tau = g/k \qquad (3.2\text{-}7)$$

in which P is the total (summation of gas and radiation) pressure and the surface gravity g is given by

$$g = GM/R^2.$$

The boundary condition for this atmospheric equation is

$$P_g(\tau=0) = 0$$

or

$$P(\tau=0) = P_{rad.}(\tau=0)$$

$$= a/3\ T^4(\tau=0) \qquad (3.2\text{–}8)$$

Integrating the equation (3.2-7) in the range $0 \leq \tau \leq \underline{\tau}$ finally gives the surface effective pressure at the photosphere;

$$P(\underline{\tau}) = \int_0^{\underline{\tau}} \frac{g}{k}\, d\tau$$

$$= P(R, L, \underline{\tau}) \qquad (3.2\text{-}9)$$

Special forms of the atmospheric equations (3.2-5) and (3.2-9) have been defined by Eddington (see 18) and Stein(20). Eddington's approximation defines temperature in the atmosphere as;

$$T^4 = 3/4\ L/(4\pi\sigma R^2)\ (\tau + 2/3)$$

which fulfill the equation (3.2-6). Robert F. Stein (20) has suggested

$$P(\underline{\tau}) = 2/3\ (a+1)\ g/k$$

where a is a constant related to the pressure or density dependence of the opacity and k is the local opacity.

Equations (3.2-6) and (3.2-9) which define the pressure and temperature at the photosphere as functions of radius and luminosity of the star determine the outer boundary conditions. Just below the photosphere the condition is more similar to the

atmospheric condition than the interior. We may, efficiently, use the atmospheric integration up to a mass $M_r = M_F < M$ which can be a fitting point to match the interior solution (for $M_r \leq M_F$) and the outer layer, atmospheric, integration (for $M_r \geq M_F$). $P(\tau)$, $T(\tau)$, R, and L can be the initial values for the outer layer integration where a sufficient number of these solutions define relations between P, T, r, and L_r at the point M_F. These relations which may be written in the general forms

$$B_1 = P-\Phi(L,r) = 0$$

$$B_2 = T-\Psi(L,r) = 0 \qquad (3.2\text{-}10)$$

can be considered as the outer boundary conditions (at M_F) for the interior solution. The value of M_F is estimated which usually is used as $M_F = 0.97M$.

The surface boundary conditions (3.2-10) can be obtained by the triangle method. Full details of this method about the conditions and the check of their validity are given by Kippenhahn et al. (18). We may rewrite the linear relations (3.2-10) as ;

$$P = a_p L_r + b_p r + c_p$$

$$T = a_t L_r + b_t r + c_t \qquad (3.2\text{-}11)$$

After differentiating and replacing by difference equations we have

$$\Delta P = a_p \Delta L + b_p \Delta r$$

$$\Delta T = a_t \Delta L + b_t \Delta r. \qquad (3.2\text{-}12)$$

The coefficients of these equations can be simply written as

$$a_p = (\Delta P/\Delta L)_r \,,\; b_p = (\Delta P/\Delta r)_L$$

$$a_t = (\Delta T/\Delta L)_r \,,\; b_t = (\Delta T/\Delta r)_L \qquad (3.2\text{-}13)$$

in which the subscripts denote the derivatives at the constant r(=R) and L_r(=L).We can use P(τ), T(τ), L, and R in the equations (3.2-11) to obtain c_p and c_t. To specify the relations (3.2-10) we need to know the coefficients defined by the expressions (3.2-13) and in (3.2-11).We can determine these coefficients in three cases by the following procedure:

1-Estimate initial values of L and R and integrate (or solving) the atmospheric equations (3.2-6) and (3.2-9) to obtain P and T.

2-A second set of estimated values L and R+ΔR are used to integrate the atmospheric equations and obtain $P+\Delta_1 P$ and $T+\Delta_1 T$.

3- Finally a third set may be defined by L+ΔL and R giving $P+\Delta_2 P$

and $T+\Delta_2 T$.

By subtracting the cases 2 and 3 from 1, we can determine $\Delta_1 P$, $\Delta_1 T$, $\Delta_2 P$, and $\Delta_2 T$.We may now write the constants (3.2-13) as;

$$(\Delta P/\Delta r)_L = \Delta_1 P/\Delta r = b_p$$

$$(\Delta T/\Delta r)_L = \Delta_1 T/\Delta r = b_t$$

$$(\Delta P/\Delta L)_R = \Delta_2 P/\Delta L = a_P$$

$$(\Delta T/\Delta L)_R = \Delta_2 T/\Delta L = a_t$$

c_p and c_t can be obtained as mentioned above. We have found now the boundary condition (3.2-10) or (3.2-11) as

$$P(M=M_F) = (\Delta_2 P/\Delta L)L_r+(\Delta_1 P/\Delta r)r+P(\tau)-(\Delta_2 P/\Delta L)L-(\Delta_1 P/\Delta r)R$$

$$T(M=M_F) = (\Delta_2 T/\Delta L)L_r+(\Delta_1 T/\Delta r)r+T(\tau)-(\Delta_2 T/\Delta L)L -(\Delta_1 T/\Delta r)R$$

The values of R and L or correspondingly T_{eff} and L in each case (1-2-3) can be one corner of a triangle in the T_{eff}, L plane. In order to keep the surface condition (3.2-10) valid our (T_{eff}, L) point have to be kept inside this triangle.

In our computer code (TRC/KWH) the outer boundary condition is applied at the photosphere where

$$L = 4\pi R^2 \sigma T^4$$

($\mathfrak{x}$=2/3), although Kippenhahn, Weigert, and Hofmeister (18) have suggested M_F=0.97M.

The behaviour of the variables near the centre have to satisfy the condition of M_c=0 and therefore r_c=L_c=0. Applying series expansions to (3.1-10) through (3.1-13) and neglecting higher order of M_r, which near the centre is approximately zero, we will have

$$r = (3/4\pi\rho_c)^{1/3}\ M_r^{1/3} \qquad (3.2\text{-}14)$$

$$P = P_c\text{-}1/2\ \ G(4\pi/3)^{1/3}\ \rho_c^{4/3} M_r^{2/3} \qquad (3.2\text{-}15)$$

$$L_r = (\varepsilon\ -T\partial s/\partial t)_c M_r \qquad (3.2\text{-}16)$$

$$T = T_c\text{-}1/2\ \ G(4\pi/3)^{1/3}\ \rho_c^{4/3}\ T_c P_c^{-1}\ \nabla_c\ M_r^{2/3} \qquad (3.2\text{-}17)$$

Subscript c denotes the values of the quantities at the centre (of course, if the central zone is convective ∇_c will be the value of $\nabla_{conv.}$). In the neighbourhood of the centre equations (3.1-10) to (3.1-13) can be replaced by these equations.

We may eliminate P_c and T_c with the assumption of that ρ_c, ∇_c,

and etc are known functions of P_c and T_c to reduce these equations to two functions with general forms

$$f_1(P, T, r, L_r) = 0$$

$$f_2(P, T, r, L_r) = 0. \qquad (3.2\text{-}18)$$

These two relations must be fulfilled by the interior solutions at a point $M=M_s$ in the neighbourhood of the centre and may be used as the central conditions.

3.3- METHOD OF CALCULATIONS

3.3-1 INTRODUCTION

In order to calculate the stellar structure, our basic problem is to solve the differential equations of (3.1-10) through (3.1-14). The solution in a model of given mass and given chemical composition is for the four dependent variables (P, T, r, L_r) at various points of the star and different times. In fact a model is solved when we have a set of tables of the physical variables and chemical composition at the selected points and times in the star.

In general the equations will be solved by some form of

numerical iteration by specific computing codes. In addition to the four dependent variables, the equations also contain a number of parameters and well-known constants. In a stellar structure and evolution code a number of subroutines will compute the parameters. These subroutines may be the calculation of the equation of state, the opacity, the nuclear energy generation, and the entropy from the local thermodynamic conditions. As in the iteration process when the value of the four variables and the X_{ij} (j represents the selected point) are given at a point, we need the parameters ρ, k, ε, s, and $\nabla_{conv.}$ for the next step.

Some parameters can be found by both direct computation from the complicated formula or by tabulated numerical values. The thermodynamic quantities ∇_{ad}, c_p, and s can be determined by the standard thermodynamical formulas. The determination of ρ for given P and T (and chemical composition) requires using the equation of state. Kippenhahn et al.(1967-18) have investigated the solution of the equation of state and the determination of density in the both ionization and degeneracy cases. In some parameters (e.g.

ρ) the derivatives are also required and in these instances it may be helpful to use a numerical evaluation.

Once a code gives P, T, r, and L_r at time t_0 regarding to $X_i(t_0)$, $\varepsilon_k(t_0)$, and $s(t_0)$ then the problem of the stellar evolution is to compute the variables for a future time $(t_0+\Delta t)$ using new X_i, ε_k, and s.

A number of numerical methods have been proposed to solve the stellar structure and evolution equations, (3.1-10) to (3.1-14). The two general methods are firstly the fitting point method, which is the integration step by step from one of the boundary points, and secondly the Henyey method, which is described by a series of concentric shells in which the first order differential equations are replaced by a system of difference equations.

Integration from one of the boundary points will reach a divergence near the other point. Schwarzschild (1958-10) has developed a procedure for fitting together the inward integration from the surface and the outward integration from the centre at an intermediate point. One can integrate the equations from both

boundaries to a preselected point and compare the solutions. When the dependent variables match at this point

$$r_{if} = r_{ef}, L_{if} = L_{ef}, P_{if} = P_{ef}, T_{if} = T_{ef}$$

then a correct model will be achieved. The subscript if and ef represent the interior integration from the centre and the exterior from the surface.

3-3.2 HENYEY CODE

The Henyey code for calculating stellar structure operates on the principle of iterative procedure in which an approximate initial solution is estimated, then the corrections to the physical variables are obtained by solving a system of linear equations. When these corrections are applied a new estimate for the stellar model is obtained and the process is repeated until the corrections become small enough to satisfy some convergence criterion.

For example consider the solution of the equation:

$$dy/dx = f(x,y). \qquad (3.3\text{-}1)$$

The initial value or boundary condition for this equation is

$$y(x=0) = y_0$$

The range of x is $0 \leq x \leq x_{max}$ and this range can be divided into zones by selecting n specific points

$$x_1, x_2, \ldots, x_{n-1}, x_n \qquad (x_j, j=1,n)$$

$$=0 \qquad\qquad =x_{max}$$

The initial values of y at these distinct points can be estimated in a table. We define these values as y_j^0 (j=1,n) which superscript 0 denotes the first estimation of the solution.

The differential equation (3.3-1) can simply be replaced by a difference equation using the difference operator Δ in place of differential operator d

$$\Delta y/\Delta x = (y_{j+1}-y_j)/(x_{j+1}-x_j)$$

$$= f(x_{j+1/2}, y_{j+1/2})$$

where

$$x_{j+1/2} = (x_{j+1}+x_j)/2$$

$$y_{j+1/2} = (y_{j+1}+y_j)/2 \qquad (3.3\text{-}2)$$

Now we have

$$(y_{j+1}-y_j)/(x_{j+1}-x_j) = f_{j+1/2}$$

or

$$(y_{j+1}-y_j)-(x_{j+1}-x_j)\, f_{j+1/2} = 0 \qquad (3.3\text{-}3)$$

in place of (3.3-1) in which

$$f_{j+1/2} = f(x_{j+1/2}, y_{j+1/2}).$$

Equation (3.3-3) concerning our first estimation (y_j^0), of course, is not valid and the difference is a value, say $E_k^0(y_j^0) \neq 0$

$$(y_{j+1}^0-y_j^0)-(x_{j+1}-x_j)f_{j+1/2}^0 = E_k^0(y_j^0) \qquad (3.3\text{-}4)$$

where

$$f_{j+1/2}^0 = f(x_{j+1/2}, y_{j+1/2}^0)$$

and k = 1, 2, . . ., n.

The problem is now to find those values of y at which (3.3-3) is satisfied or

$$E_k^{(i)}(y_1^{(i)}, \ldots\ldots\ldots, y_n^{(i)}) = 0 \qquad (3.3\text{-}5)$$

$$k=1,n$$

where

$$E_k^{(i)}(y_j^{(i)})$$

is defined as in (3.3-4) and superscript i denote the order of the

iteration.

At first Newton derived a geometrical method for this problem (see 16 for more details): finding the corrections δy_j for estimated values of y_j which give the corrections δE_k for $E_k^{(i)}(y_j^{(i)})$ to vanish. For our first estimation we have

$$E_k^0(y_j^0)+\delta E_k = 0 \qquad (3.3\text{-}6)$$

$$\delta E_k = \sum_{j=1}^{n} \left(\frac{dE_k}{dy_j}\right)^0 \delta y_j$$

$$k = 1, \ldots, n$$

in which the superscript 0 denotes that the derivatives have to be taken for the values y_j^0. These simply give the corrections which enable us to have better approximations

$$y_0^{(1)} = y_0^0 = y_0$$

$$y_1^{(1)} = y_1^0+\delta y_1$$

$$y_2^{(1)} = y_2^0+\delta y_2 \qquad (3.3\text{-}7)$$

. . .

. . .

. . .

$$y_j^{(1)} = y_j^0 + \delta y_j$$

The new values are then introduced into the functions (3.3-5) where the $E_k^{(i)}(y_j^{(i)})$ are changed by the amount of δE_k and the process will be repeated until the corrections δy_j become as small as possible. Then we have found the actual solutions $y_j^{(s)}$ after i=s iterations.

We have summarized the entire process into the following chart

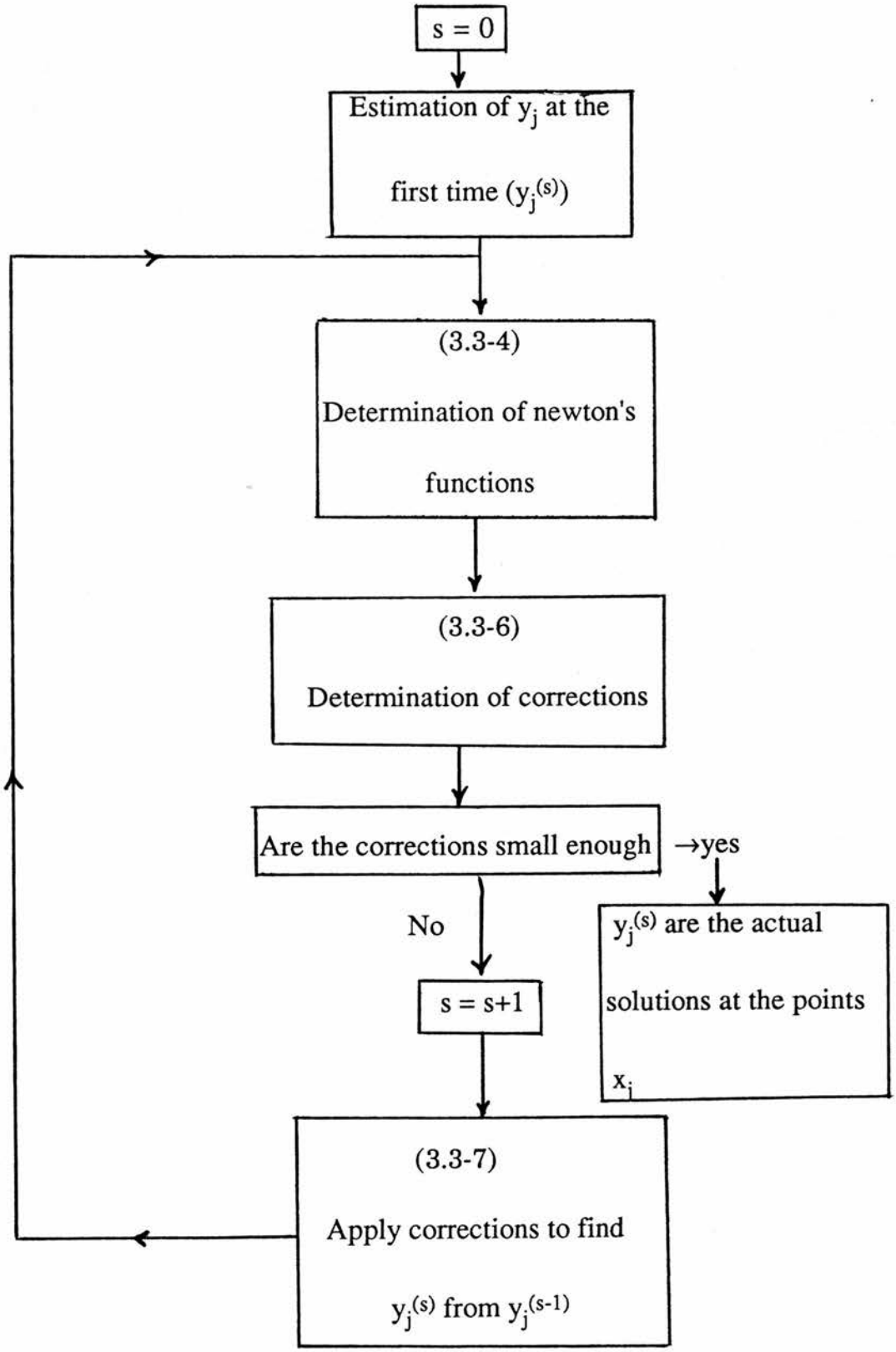
s = 0
Estimation of y_j at the first time ($y_j^{(s)}$)
(3.3-4)
Determination of newton's functions
(3.3-6)
Determination of corrections
Are the corrections small enough
→yes
No
$y_j^{(s)}$ are the actual solutions at the points x_i
s = s+1
(3.3-7)
Apply corrections to find $y_j^{(s)}$ from $y_j^{(s-1)}$

For the stellar evolution we have followed the prescription given by Kippenhahn, Weigert, and Hofmeister (1967). M (stellar mass) ranging from $M_0=M$ at the surface to $M_n=0$ at the centre and the star can be divided into n concentric shells

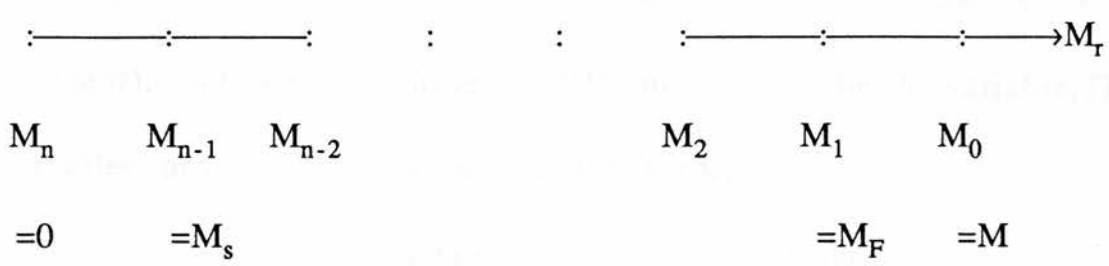

Since all variables in a stellar model range over several orders of magnitude we may use more convenient forms of them by suitable transformations. The independent variable, M_r, can be replaced by

$$x = \log\{1-M_r/[(1+\eta)M]\} \qquad (3.3\text{-}8)$$

and the dependent (unknown) ones by

$$p = \log(P),\ \vartheta = \log(T),\ h = \log(r),\ l=\log(L_r) \qquad (3.3\text{-}9)$$

in the interval $M_s \leq M_r \leq M_F$. For the outer layer integrations ($M_r>M_F$) which are carried from the top of the atmosphere inward to the layer $M_r=M_F$ transformation (3.3-8) is in a suitable form with

$0<\eta\ll 1$, otherwise for above mentioned range of M_r, η can be zero $(0\leq\eta\ll 1)$ to define

$$q = \log[1-M_r/M]. \qquad (3.3\text{-}10)$$

Although for the central zone we may use $l=\log(1+L_r/L')$ (L' is a constant), but we still have a difficulty with the h variable.The variables now are transformed to the forms

$$x = x(M_r) \qquad \text{known}$$

$$p = p(P),\ \vartheta = \vartheta(T),\ h = h(r),\ l = l(L_r) \qquad \text{unknown} \quad (3.3\text{-}11)$$

All variables and parameters distributed in the zones are to be defined in the form (3.3-2), except ε which is highly temperature sensitive and consequently the average of ε at the two boundaries of a zone is not a good approximation, so it has been suggested

$$\varepsilon_{j+1/2} = (\varepsilon_j\ \varepsilon_{j+1})^{1/2}$$

3.3-3 DIFFERENCE EQUATIONS

We may rewrite the system of equations (3.1-10) through (3.1-13) applying the transformation (3.3-11) and replacing the system with difference equations

$$\frac{h_{j+1}-h_j}{x_{j+1}-x_j} = \frac{1}{4\pi r^2_{j+1/2}(h)\,\rho_{j+1/2}(p,\vartheta,X_i)} \frac{(\frac{dh}{dr})_{j+1/2}}{(\frac{dx}{dM_r})_{j+1/2}} \qquad (3.3\text{-}12a)$$

$$\frac{p_{j+1}-p_j}{x_{j+1}-x_i} = -\frac{G\,M_{r_{j+1/2}}(x)}{4\pi r^4_{j+1/2}(h)} \frac{(\frac{dp}{dP})_{j+1/2}}{(\frac{dx}{dM_r})_{j+1/2}} \qquad (3.3\text{-}12b)$$

$$\frac{l_{j+1}-l_i}{x_{j+1}-x_i} = [\,\varepsilon_{j+1/2}-T_{j+1/2}(\vartheta)\,\frac{s_{j+1/2}-s'_{j+1/2}}{\Delta t}] \frac{(\frac{dl}{dL_r})_{j+1/2}}{(\frac{dx}{dM_r})_{j+1/2}} \qquad (3.3\text{-}12c)$$

$$\frac{\vartheta_{j+1}-\vartheta_j}{x_{j+1}-x_j} = -\frac{GM_{r_{j+1/2}}(x)\,T_{j+1/2}(\vartheta)}{4\pi r^4_{j+1/2}(h)\,P_{j+1/2}(p)}\,\nabla_{j+1/2}(p,\vartheta,l,x) \frac{(\frac{d\vartheta}{dT})_{j+1/2}}{(\frac{dx}{dM_r})_{j+1/2}}$$

(3.3-12d)

where s' is the entropy at the time t_0 , Δt is the time step of stellar evolution and subscript $j+1/2$ for derivatives denotes that the derivatives have to be taken between two meshpoints j and j+1.

The interval $M_s \le M_r \le M_F$ is divided into n-2 mass shells by the points $M_1(=M_F)$, M_2, . . ., $M_{n-1}(=M_s)$ which correspond to the meshpoints x_1, x_2, . . ., x_{n-1}. Each of n-2 mass shells gives four difference equations of (3.3-12) with the general form

$$G_i(p_j, \vartheta_j, h_j, l_j, p_{j+1}, \vartheta_{j+1}, h_{j+1}, l_{j+1}) = 0 \qquad (3.3\text{-}13)$$

$$(i=1,4\ ;\ j=1,n-2)$$

We can write out the difference equations G_i using the transformation (3.3-11)

$$G_1=(h_{j+1}-h_j)-(x_{j+1}-x_j)\frac{1}{4\pi\rho_{j+\frac{1}{2}}}10^{-3h_{j+1/2}}[10^{x_{j+1/2}}-(1+\eta)M] \qquad (3.3\text{-}14)$$

$$G_2=(p_{j+1}-p_j)+(x_{j+1}-x_j)\frac{G}{4\pi}10^{(x_{j+1/2}-p_{j+1/2}-4h_{j+1/2})}[10^{x_{j+1/2}}-(1-\eta)M]$$

$$G_3=(l_{j+1}-l_j)-(x_{j+1}-x_j)(\varepsilon_{j+1/2}-10^{\vartheta_{j+1/2}}\frac{s_{j+1/2}-s'_{j+1/2}}{\Delta t}10^{-1}[10^{x_{j+1/2}}-(1+\eta)M]$$

$$G_4=(\vartheta_{j+1}-\vartheta_j)+(x_{j+1}-x_j)\frac{G}{4\pi}10^{(x_{j+1/2}-p_{j+1/2}-4h_{j+1/2})}\nabla_{j+1/2}[10^{x_{j+1/2}}-(1+\eta)M]$$

where η is in the range $0\leq\eta\ll 1$ and

$$h_{j+1/2} = (h_{j+1}+h_j)/2$$

$$x_{j+1/2} = (x_{j+1}+x_j)/2$$

$$\rho_{j+1/2} = (\rho_{j+1}+\rho_j)/2$$

$$p_{j+1/2} = (p_{j+1}+p_j)/2 \qquad (3.3\text{-}15)$$

$$\varepsilon_{j+1/2} = (\varepsilon_{j+1}\cdot\varepsilon_j)^{1/2}$$

$$\vartheta_{j+1/2} = (\vartheta_{j+1}+\vartheta_j)/2$$

$$s_{j+1/2} = (s_{j+1} + s_j)/2$$

$$l_{j+1/2} = (l_{j+1} + l_j)/2$$

$$\nabla_{j+1/2} = (\nabla_{j+1} + \nabla_j)/2$$

and M is the total mass of the star. All these 4(n-2) equations stand against the 4(n-1) unknowns p_j, ϑ_j, h_j, l_j (j=1,n-1). Further equations must be obtained from the boundary conditions.

Applying the transformation (3.3-11) in the outer boundary conditions (3.2-10) at $x_1(=M_F)$ we have

$$B_1(p_1, \vartheta_1, h_1, l_1) = 0$$

$$B_2(p_1, \vartheta_1, h_1, l_1) = 0 \qquad (3.3\text{-}16)$$

At the centre where P_c and T_c are also of interest we prefer to work with the equations (3.2-14) to (3.2-17). Using these equations at the x_{n-1} $(=M_s)$ and applying the transformation, we will have four equations with the general form

$$C_i(p_{n-1}, \vartheta_{n-1}, h_{n-1}, l_{n-1}, p_n, \vartheta_n) = 0 \qquad (3.3\text{-}17)$$

$$(i=1,4)$$

where

$$p_n = \log(p_c)$$

$$\vartheta_n = \log(T_c)$$

Equations (3.3-13), (3.3-16), and (3.3-17) now give us as many equations as unknowns (p_j, ϑ_j, h_j, l_j, j=1,n-1 ;p_n, ϑ_n) which can be solved by Newton's method.

3.3-4 SOLUTION OF THE DIFFERENCE EQUATIONS

If p_j^0, ϑ_j^0, h_j^0, and l_j^0 make the first approximated solution then we will need corrections δp_j, $\delta \vartheta_j$, δh_j, and δl_j to improve the estimation. The equations (3.3-6) show that these corrections are given by the linear equations

$$dB_k/dp_1\ \delta p_1 + dB_k/d\vartheta_1\ \delta\vartheta_1 + dB_k/dh_1\ \delta h_1 + dB_k/dl_1\ \delta l_1 = -B_k \quad (3.3\text{-}20a)$$

$$k=1,2$$

$$dG_i/dp_j\ \delta p_j + dG_i/d\vartheta_j\ \delta\vartheta_j + dG_i/dh_j\ \delta h_j + dG_i/dl_j\ \delta l_j + dG_i/dp_{j+1}\ \delta p_{j+1}$$

$$+dG_i/d\vartheta_{j+1}\ \delta\vartheta_{j+1} + dG_i/dh_{j+1}\ \delta h_{j+1} + dG_i/dl_{j+1}\ \delta l_{j+1} = -G_i \quad (3.3\text{-}20b)$$

$$(i=1,4\ ;\ j=1,n-2)$$

$$dC_i/dp_{n-1}\ \delta p_{n-1} + dC_i/\delta\vartheta_{n-1}\ \delta\vartheta_{n-1} + dC_i/dh_{n-1}\ \delta h_{n-1} + dC_i/dl_{n-1}\ \delta l_{n-1}$$

$$+dC_i/dp_n\ \delta p_n\ +dC_i/d\vartheta_n\ \delta\vartheta_n = -C_i \qquad (3.3\text{-}20c)$$

$$(i=1,4)$$

The coefficient of these equations and the functions on the right, can be calculated from the values of the approximated solutions with the parameters X_i, s', and Δt by the equations (3.3-13) or (3.3-14), (3.3-16), and (3.3-17) . The system of equations (3.3-20) which can be written in the matrix form

$$\begin{bmatrix} \frac{dB_1}{dp_1} & & \\ \vdots & & \\ & \cdots & \frac{dC_4}{d\vartheta_n} \end{bmatrix} \begin{bmatrix} \delta p_1 \\ \vdots \\ \delta\vartheta_n \end{bmatrix} = \begin{bmatrix} -B_1 \\ \vdots \\ -C_4 \end{bmatrix} \qquad (3.3\text{-}21)$$

is solvable for 4n-2 corrections and the new approximations are

$$\begin{aligned} p_1^{(1)} &= p_1^0 + \delta p_1 \\ \vartheta_1^{(1)} &= \vartheta_1^0 + \delta\vartheta_1 \\ &\vdots \\ \vartheta_n^{(1)} &= \vartheta_n^0 + \delta\vartheta_n \end{aligned} \qquad (3.3\text{-}22)$$

If the corrections are not small enough the new variables must be

used in place of the initial ones

$$(p_i^0, \vartheta_j^0, h_j^0, l_j^0 \; ;j=1,n-1 \quad , p_n^0, \vartheta_n^0)$$

and the process continues until corrections are as small as possible or the errors limit the convergence and the process stops.

3.3-5 GENERAL DETAILS

Following the equations (3.2-11) for the outer boundary integration we need to estimate L and T_{eff} as we need initial approximate solutions for the interiors. In the case of the first model of an evolutionary sequence or zero age main sequence, i. e., where stars are homogeneous, where X_i are constant, and where evolution is quite slow then the approximation of $T\,\partial s/\partial t = 0$ can be used in the equations (3.1-3), (3.1-12), (3.3-12c), and (3.3-14c). In such this case a standard zero age model with the same or different mass and composition is usually sufficient to provide an approximate solution. When evolution takes place the result of this case can be used for the next stage, as the solution of the model at the time t is a good initial approximation for the time $t+\Delta t$. An easier example is when zero age main sequence models of different masses are computed by the same program using the same subroutines for the parameters. In this case a normal program can be used setting

$$\partial s/\partial t = \partial X_i/\partial t = 0$$

and using each of these models at the start, when calculating other homogeneous models of different mass.

Once an approximate solution is established, surface conditions appropriate to it are obtained in the form (3.3-16). Coefficients for the equation (3.3-21) are established so that the system is solved for the corrections δp_1, ..., $\delta \vartheta_1$, then these corrections can be applied to the approximate solution, and the procedure is repeated. The program interrupts iteration as soon as the corrections decrease below a certain limit but the problem is to have a good convergence of the corrections. To check the convergence, the values of the computed corrections have to be checked. One can multiply all corrections by a constant $\alpha \leq 1$ before applying them (the value of α depends on the size of the corrections). Of course α is less than one for corrections above a certain limit and its value will be controlled (changed) during the iteration process. In our work the initial value for α has been taken 1 and the convergence limit for the r.m.s. of the corrections is 10^{-5} as there is an emergency stop when corrections become too large or when there is no hope for convergence due to any error. The choice of the initial approximate

solution is also important in reaching the convergence limit as soon as possible. As a large time step may cause divergence and the small Δt will waste computer time so we need to check Δt during the process.

In order that the difference equations approximate the differential equations the stepwidths in all variables must be sufficiently small. However, because of the limitation of storage space and the time taken by the computer, the mass shells should not be too small. To satisfy both these conditions there is a scheme detailed by Kippenhahn et al. (18) starting with the criteria

$$\begin{aligned}
\Delta p_{min} < \Delta p < \Delta p_{max} \qquad & \Delta p = |p_{j+1} - p_j| \\
\Delta \vartheta_{min} < \Delta \vartheta < \Delta \vartheta_{max} \qquad & \Delta \vartheta = |\vartheta_{j+1} - \vartheta_j| \\
\Delta h_{min} < \Delta h < \Delta h_{max} \qquad & \Delta h = |h_{j+1} - h_j| \\
\Delta l_{min} < \Delta l < \Delta l_{max} \qquad & \Delta l = |l_{j+1} - l_j| \qquad (3.3\text{-}23) \\
\Delta x_{min} < \Delta x < \Delta x_{max} \qquad & \Delta x = |x_{j+1} - x_j| \\
\Delta X_{i_{min}} < \Delta X_i < \Delta X_{i_{max}} \qquad & \Delta X_i = |X_{i_{j+1}} - X_{i_j}|
\end{aligned}$$

The minimum and maximum of the variables are input parameters

and can easily be changed. Each mass shell has to satisfy (3.3-23), if one or more of the right hand inequalities is violated a new meshpoint is inserted at a point defined by $x = x_{j+1/2}$. For the left hand ones the mesh point x_{j+1} is deleted.

Finally we summarize the overall scheme for the entire program in the following flow chart:

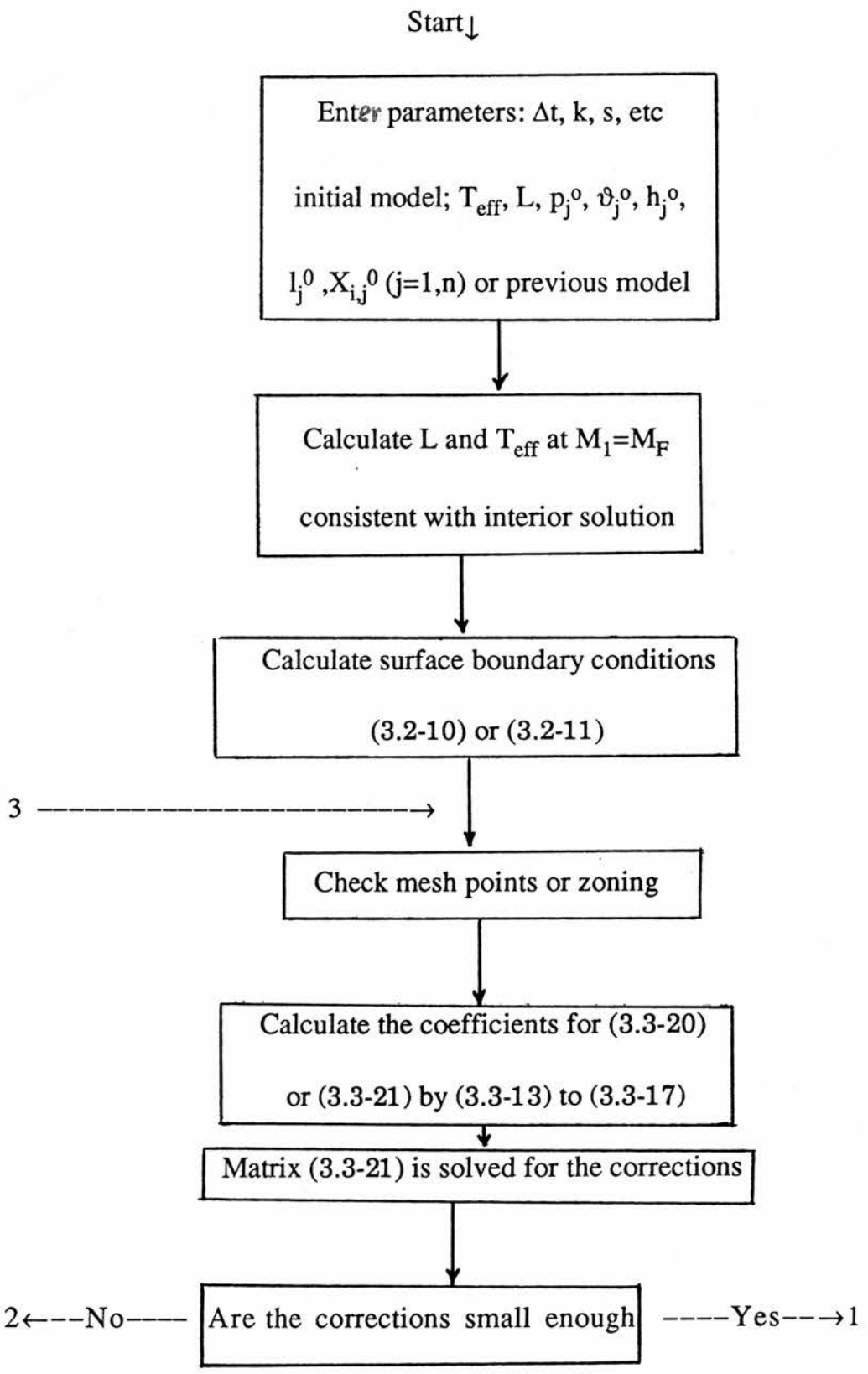
Start
Enter parameters: Δt, k, s, etc
initial model; T_{eff}, L, p_j^o, ϑ_j^o, h_j^o,
l_j^0 ,$X_{i,j}^0$ (j=1,n) or previous model
Calculate L and T_{eff} at $M_1=M_F$
consistent with interior solution
Calculate surface boundary conditions
(3.2-10) or (3.2-11)
3
Check mesh points or zoning
Calculate the coefficients for (3.3-20)
or (3.3-21) by (3.3-13) to (3.3-17)
Matrix (3.3-21) is solved for the corrections
2←No
Are the corrections small enough
Yes→1

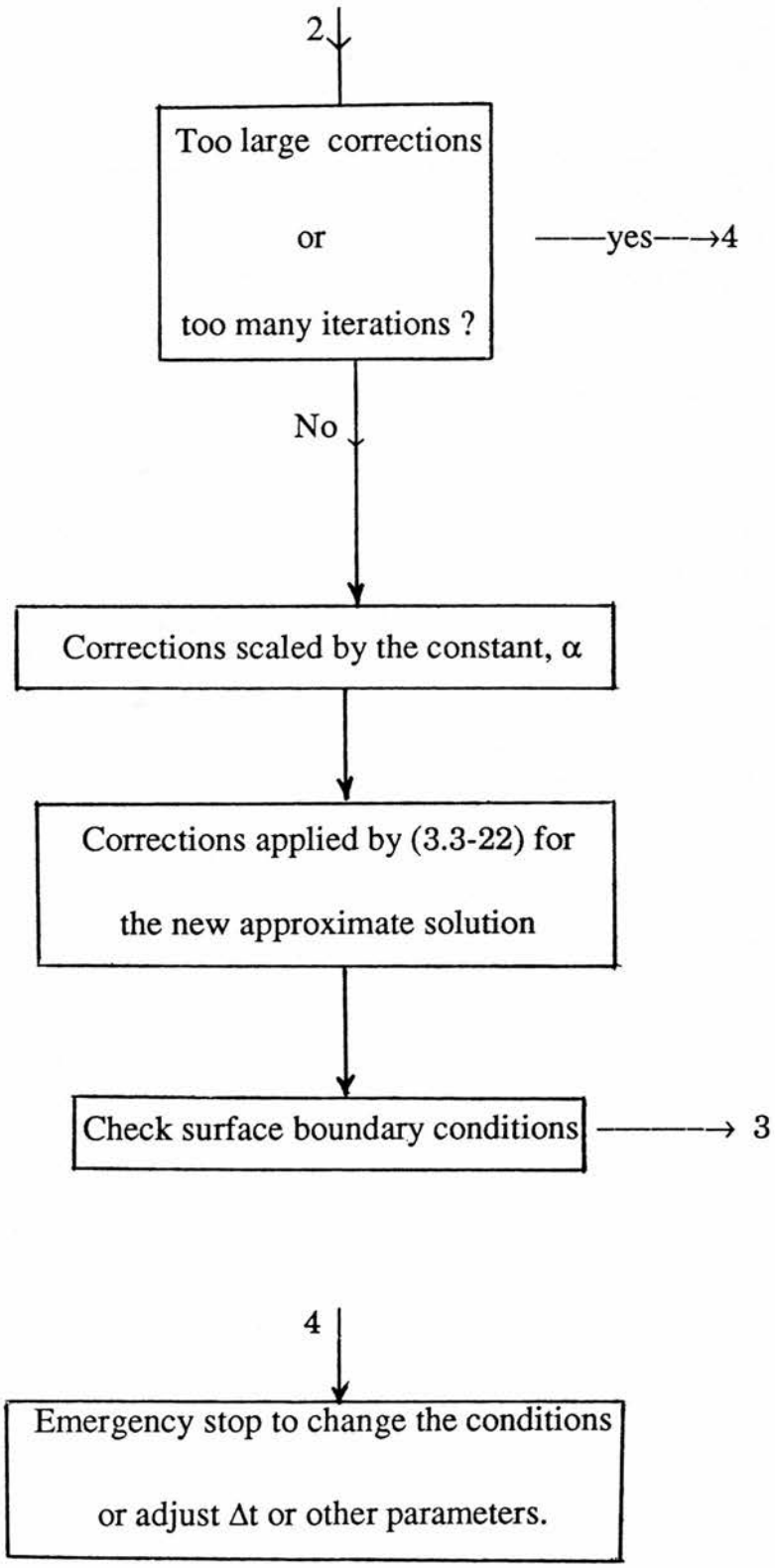
2
Too large corrections
or
too many iterations ?
yes→4
No
Corrections scaled by the constant, α
Corrections applied by (3.3-22) for
the new approximate solution
Check surface boundary conditions
→ 3
4
Emergency stop to change the conditions
or adjust Δt or other parameters.

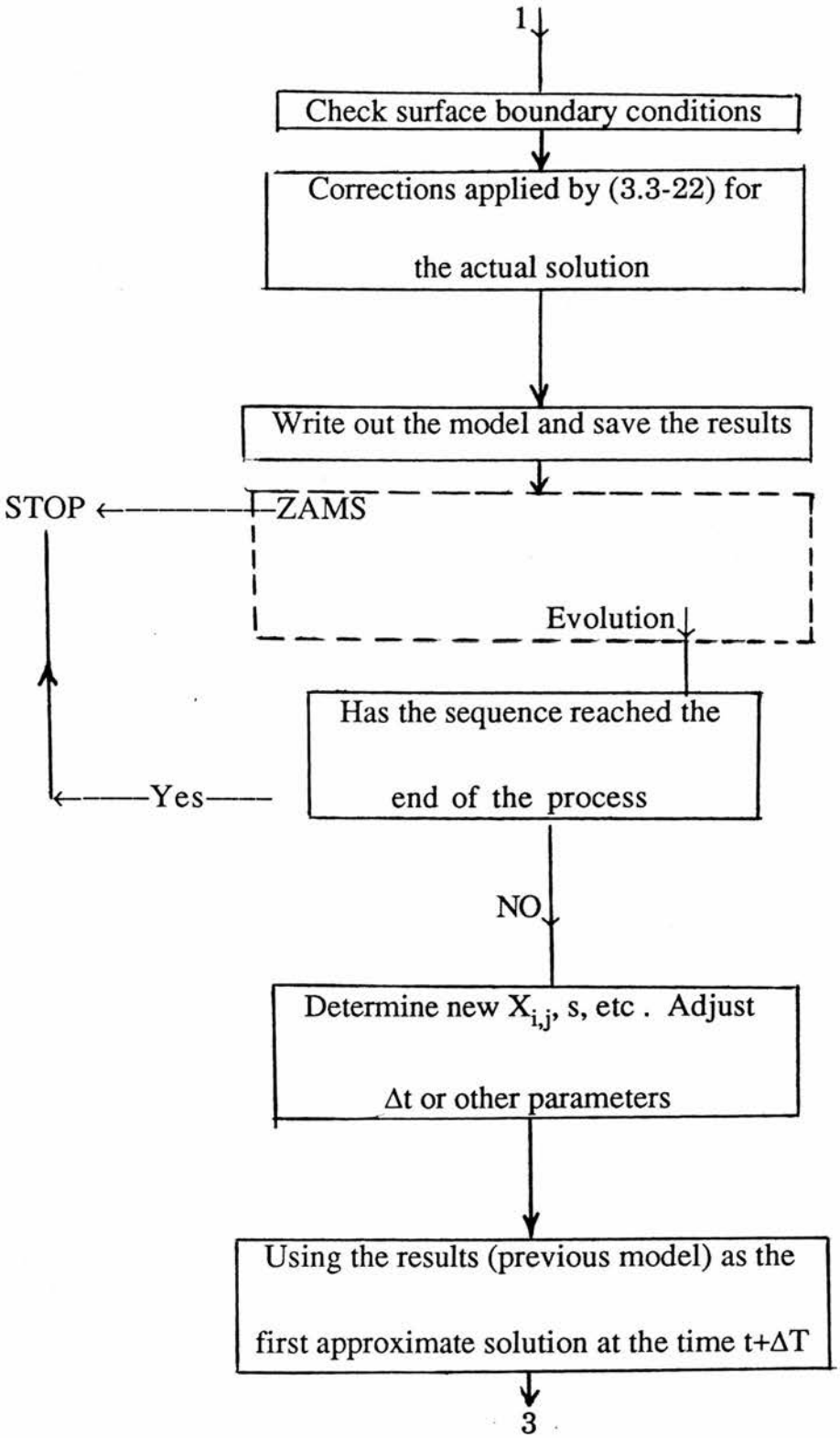
1
Check surface boundary conditions
Corrections applied by (3.3-22) for the actual solution
Write out the model and save the results
STOP
ZAMS
Evolution
Has the sequence reached the end of the process
Yes
NO
Determine new $X_{i,j}$, s, etc . Adjust Δt or other parameters
Using the results (previous model) as the first approximate solution at the time t+ΔT
3

4- M-S EVOLUTION AND LOWER ZAMS MODELS

4-1 INTRODUCTION

Stars are believed to form from diffuse interstellar clouds. As the interior temperature of a new born gravitationally contracting star rises, the star moves down the Hayashi track to the main sequence. When the central temperature of the star becomes high enough to burn hydrogen, the star enters its main sequence hydrogen burning phase, the longest stage of its life time. The luminosity of the star begins to be supported by the thermonuclear conversion of hydrogen to helium. The central temperature, which depends on the mass of the star, determines the mode of energy production (P-P or C-N cycle) and this in turn (see Section 2.2) determines the length of the main sequence life-time of the star.

Once a star arrives at the main sequence, and starts burning hydrogen in the core, it remains there for a long time. The locus of the luminosity versus the effective surface temperature of such stars define the zero age main sequence (ZAMS) stage in the H-R diagram. Hereafter the star's homogeneous composition will begin to change which causes a change in the position of the star on the H-R diagram. thus the structure of the star differs in each part of the diagram and different parts define the location of different

types of stars. The evolutionary track of a star shows the behaviour of its internal structure while the star evolves.

When the hydrogen in the core is exhausted and transformed into helium, the core of the star contracts and heats up. The star undergoes a brief period of overall contraction and its track makes a blueward movement which is evident in higher mass tracks. The rising temperature enables hydrogen thermonuclear reactions to occur in a hydrogen shell source surrounding the core. A star in this stage is composed of a helium core, a hydrogen burning shell, and a hydrogen envelope. The hydrogen burning at first occurs in a thick-shell followed by a shell-narrowing phase (see e.g. 23). Iben (23) has noted that the life time of the thick-shell phase is relatively large and increases with decreasing stellar mass.

The evolution during later phases may depend critically on the evolution during the main-sequence life time. This is, as mentioned by T. J. Van der Linden(1986-24), due to the "integrated effects" in the main-sequence evolution. As the shell is narrowing the core continues to contract and heat up, until at the tip of the giant branch (see 23 and 25) the temperature becomes high enough for helium burning and so helium starts to burn in the core. Even so, the results of J. G. Mengel et al. (1979-26) show that a few

sequences with large M(mass) and low Z start central helium burning before the tracks reach the red-giant branch. B. Paczynski (1969-27) reported that a model of $15M_{\odot}$ with Z=0.03 spent all the core helium burning phase in the red giant region. However, the star settles again into a relatively stable phase for a considerable time in regard to the shell helium burning (after the exhaustion of helium in the core). Depending on its mass, a star may thereafter proceed to carbon, neon, and oxygen burning and it now has a completely inhomogeneous composition.

Full details about the different stages of stellar evolution are given by several authors including Iben in a series of papers. Evolutionary tracks of several metal-rich stars of various masses in different evolutionary phases are shown in Fig. 3 of Iben's (23) paper. Mengel et al. (26) have computed a set of 247 evolutionary sequences extending from the ZAMS to the base of the red-giant branch. These calculations are primarily restricted to stars of relatively low mass, although some models as massive as $6.9M_{\odot}$ are considered. Fig. 1 of their paper shows evolutionary tracks of stars for a large range of mass and composition.

The shape of the evolutionary tracks in the H-R diagram depends on the mass and composition of the star. The effect of the

initial composition on the evolution is shown by Mengel et al.(26), C. Alcock & Paczynski (1978-28), and Becker (1980-25). Becker's results show that for a given model mass the evolutionary behaviour depends strongly on its initial composition. As noted by Alcock & Paczynski the main sequence is bluer and more luminous for the low Z models because of the Kramers' part of the opacity.

The shapes of evolutionary tracks are completely different in low mass and high mass stars. For massive stars where the radiative energy transport dominates the mode of energy transport, the opacity in the interior of the star is nearly constant, so the luminosity is approximately proportional to the central temperature which is constant. Thus the track in the H-R diagram is a nearly horizontal line (see 20). According to Mengel et al. (26) the blueward movement in the tracks of massive stars is due to the sudden contraction of the star while the transition of the hydrogen burning from the core to the shell occurs abruptly. At the lower masses the core is not convective during the core hydrogen burning phase; consequently, there is a more gradual transition to the hydrogen shell burning and therefore the phase of overall contraction is absent (see also 23). Stein(20) noted that for low mass stars which are fully convective the luminosity is determined by

the boundary layer of the convective region (surface). Above this, the radiative temperature gradient drops rapidly as the density decreases so the effective temperature is nearly constant and the track is nearly a vertical line.

For wider discussion of theoretical results the reader is referred to review papers by Iben and other mentioned references.

4-2 CONSTRUCTION OF THE MODELS

We have calculated the evolutionary and non-evolutionary models for different masses and compositions. Following Chapter 2 we have summarized input physics in this section. Models are calculated using T. R. Carson's code which is the Henyey method based on the prescription of Kippenhahn et al.(18). The interiors of the stellar models are calculated with photosphere ($L=4\pi R^2\sigma T^4$) chosen as the point where the surface boundary condition is applied (fitting point). The convection is treated in the same way as Kippenhahn et al.(18) by solving for ∇ in the cubic equation given by them. In the equation of state H, He, C, N, and O are included with full ionization equilibrium for all stages of ionization. H^- as well as the pressure ionization and dissociation are also included. For lower temperature regions, formation of the most important

molecules, H_2 and CO, are also considered. For temperatures greater than 10^4 ^{0}K, the opacities are given by the R. F. Christy analytical fit to opacity tables. For lower temperatures ($T< 10^4$ ^{0}K) opacities are computed from the tables of Carson and Sharp (1988-in progress). The lower temperature opacities involve H^-, H_2, CO, H_2O, CO_2, CN, N_2, and OH. The formula used for energy generation rates are taken from Fowler et. al.(1975-29).

Evolutionary sequences for the masses in the range 2.187 to 5 solar masses with the solar composition, (X,Z)=(0.73,0.02), are presented in the next section. A set of 18 low mass main sequence (non-evolutionary) for stars of mass 0.1 to 1.0 M_Θ with composition (0.770,0.018) and (0.783,0.001) are calculated in Section 4-4. In Section 4-5 we have worked on the effect of molecules on the structure of low mass stars. Models of 0.1 -1.0 M_Θ in both population type with simple equation of state (without molecules formation) are calculated when molecular opacities are and are not ignored. In order to find the effect of the molecular equation of state we have recalculated the models presented in Section 4-4 without inclusion of molecule formation in the equation of state. Five evolutionary sequences for 1.0 M_Θ with (X,Z) = (0.770,0.018) and different case of

opacity, with α = 0.5, 1.0, 2.0 calculated by Dr. Carson are also presented to complete this investigation. Finally models are compared with observations in the last Section.

4-3 MAIN SEQUENCE EVOLUTION

We have calculated evolutionary sequences for stars of 2.187, 2.50, 3.125, 3.750, 4.375, and 5.00 solar masses. The calculations were started with homogeneous main sequence models having an initial heavy-element mass fraction Z=0.020 and an initial hydrogen content X=0.730. The evolutionary sequences extend to the beginning of the giant branch. The mixing length to pressure scale height ratio, α, is taken to be 1.0. More than half an hour of computing time is sufficient to get an evolutionary track from the ZAMS to the base of the giant branch.

The evolutionary tracks of the models on the H-R diagram are shown in Fig. 4-1. The dashed line indicates the location of the ZAMS and the numbers indicate those positions at which the behaviour of the interior structure and evolution of the star changes as it evolves. The tracks have the familiar and regular shape and the blueward movement (the so called overall contraction phase) in each track is evident. Point 1 shows the

Fig. 4-1: Evolutionary tracks of models with (X, Z)= (0.73, 0.02) which are terminated at the base of the giant branch. Dashed line indicates the ZAMS loci.

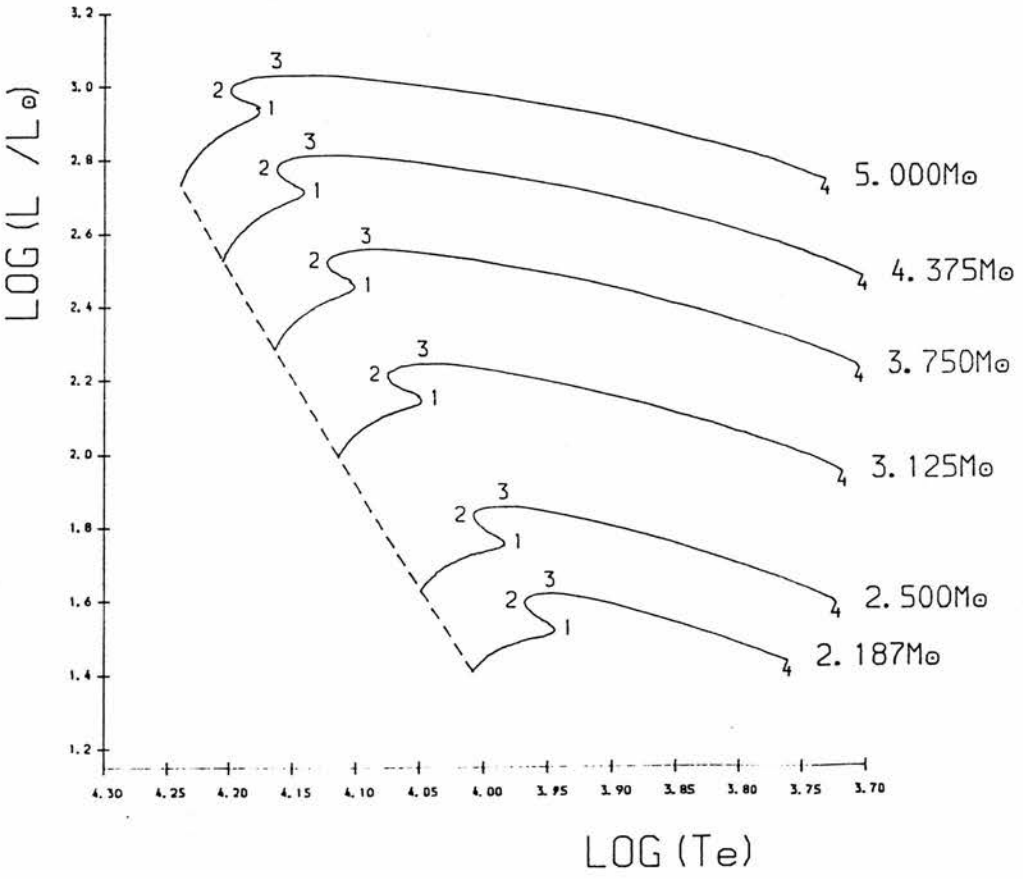

coolest (=reddest) point of the main sequence at which the core hydrogen is nearly exhausted. Point 2 is the bluest point, following point 1, which is a starting point for hydrogen burning in a thick shell. The most luminous point of a track is shown by point 3 at which the shell narrowing phase starts.

As mentioned in Section 4-1 and is evident from the Tables 4-1 to 4-6, the life time between point 1 and 2 or 1 and 3 is considerably longer than that of points 3 to 4. Therefore, there is a relatively stable phase between point 1 and 2 or 3 and this cause that some authors use point 2 or 3 as the end of the main sequence phase rather than point 1. We would like to use a general point between 1 and 2 where core exhaustion occurs, as that point. Finally the evolutionary tracks terminate at point 4 which presents the end of the shell narrowing phase that hereafter the giant phase will start. Just after the point 4 there existed an irregular drop in luminosity which is not shown in Fig. 4-1. This local minimum in the luminosity at the base of the red-giant branch is also considerably evident in Mengel et al.(26) and Becker (25).

Data on the evolutionary characteristics of each model sequence are presented in Tables 4-1 through 4-6. Column 1 for

Table 4-1: Evolution from the ZAMS up to the base of the red giant; $M=2.187M_{\odot}$, (X,Z)=(0.730,0.020). The numbers in the first column are shown in the Fig. 4-1.

t		$\log T_e$	$\log L/L_{\odot}$	$R/R_{\odot}$	X_c	Y_c	Z_c	T_c	$P_c/10^{17}$	D_c
10^7yrs		(^{0}K)						10^7K	dycm^{-2}	gcm^{-3}
0.0		4.009	1.409	1.636	0.730	0.250	0.020	2.097	1.433	51.500
03.125		4.007	1.415	1.662	0.704	0.276	0.020	2.115	1.437	54.700
06.250		4.005	1.422	1.689	0.677	0.303	0.02001	2.126	1.431	55.500
09.375		4.003	1.430	1.718	0.650	0.331	0.02001	2.139	1.424	56.380
12.500		4.001	1.437	1.749	0.621	0.360	0.02001	2.152	1.417	57.310
15.630		3.999	1.444	1.783	0.592	0.388	0.02002	2.166	1.410	58.300
18.750		3.996	1.451	1.819	0.560	0.420	0.02002	2.180	1.403	59.400
25.000		3.990	1.466	1.900	0.491	0.490	0.02003	2.207	1.381	59.700
31.250		3.982	1.479	2.001	0.413	0.567	0.02005	2.246	1.368	63.120
38.280		3.971	1.494	2.149	0.314	0.666	0.02006	2.306	1.362	68.970
45.310		3.954	1.506	2.349	0.187	0.793	0.02008	2.407	1.401	80.200
50.000	1	3.945	1.521	2.499	0.082	0.898	0.02009	2.572	1.600	98.100
51.560		3.950	1.539	2.490	0.005	0.975	0.02010	2.704	1.904	114.80
51.950		3.951	1.543	2.491	0.0	0.9801	0.01986	2.605	2.015	127.70
52.340		3.962	1.569	2.435	0.0	0.9801	0.01986	2.561	2.729	178.20
52.730	2	3.969	1.597	2.442	0.0	0.9801	0.1986	2.477	4.317	299.70
53.300		3.965	1.614	2.535	0.0	0.9801	0.01986	2.412	6.886	510.30
54.100	3	3.949	1.622	2.757	0.0	0.9801	0.01986	2.429	16.50	1330.0
54.390		3.916	1.604	3.132	0.0	0.9801	0.01986	3.024	73.77	5442.0
54.470		3.885	1.577	3.509	0.0	0.9801	0.01986	4.049	241.2	14200
54.500		3.842	1.533	4.062	0.0	0.9801	0.01986	5.467	722.2	33070
54.530	4	3.761	1.436	5.271	0.0	0.9801	0.01986	7.703	2430	82820

Table 4-2: Same as the Table 4-1 but for M = 2.50$M_\odot$

t		$\log T_e$	$\log L/L_\odot$	$R/R_\odot$	X_c	Y_c	Z_c	T_c	$P_c/10^{17}$	D_c
10^7yrs		(^{0}K)						10^7K	dycm^{-2}	gcm^{-3}
0.0		4.049	1.630	1.751	0.730	0.250	0.020	2.174	1.274	43.840
3.125		4.047	1.641	1.791	0.697	0.284	0.020	2.193	1.270	46.100
6.250		4.044	1.652	1.836	0.655	0.325	0.020	2.210	1.258	46.950
9.375		4.041	1.663	1.886	0.612	0.368	0.02002	2.229	1.246	47.960
12.50		4.038	1.674	1.943	0.571	0.409	0.02002	2.249	1.232	49.070
15.63		4.034	1.686	2.007	0.525	0.455	0.02003	2.271	1.220	50.250
18.75		4.029	1.697	2.077	0.475	0.5047	0.02004	2.295	1.208	51.850
25.00		4.016	1.718	2.257	0.358	0.622	0.02005	2.353	1.181	54.150
31.25		3.997	1.739	2.529	0.207	0.773	0.02007	2.465	1.196	63.380
32.81		3.990	1.744	2.617	0.161	0.819	0.02008	2.512	1.220	67.420
34.38		3.985	1.751	2.708	0.108	0.872	0.02009	2.590	1.292	74.560
35.16	1	3.983	1.756	2.744	0.080	0.900	0.02009	2.649	1.362	79.580
36.33		3.989	1.776	2.735	0.005	0.975	0.02010	2.819	1.653	94.810
36.72		3.998	1.794	2.671	0.0	0.980	0.01964	2.909	1.988	111.70
37.01	2	4.008	1.830	2.662	0.0	0.980	0.01964	2.585	3.626	237.50
37.50		4.002	1.853	2.815	0.0	0.980	0.01964	2.491	6.993	498.90
37.99	3	3.985	1.860	3.069	0.0	0.980	0.01964	2.540	16.49	1252.0
38.18		3.936	1.833	3.730	0.0	0.980	0.0196	3.685	125.3	7621.0
38.23		3.871	1.777	4.709	0.0	0.980	0.01964	5.680	615.9	26180
38.24		3.823	1.726	5.554	0.0	0.980	0.01964	6.980	1272.0	45330
38.25	4	3.723	1.592	7.516	0.0	0.980	0.01964	8.939	3005.0	86390

Table 4-3: Same as Table 4-1 but for M=3.125

t		$\log T_e$	$\log L/L_\odot$	$R/R_\odot$	X_c	Y_c	Z_c	T_c	$P_c/10^{17}$	D_c
10^7yrs		(^{0}K)						10^7K	dycm^{-2}	gcm^{-3}
0.0		4.114	1.995	1.976	0.730	0.250	0.020	2.297	1.030	33.140
3.125		4.110	2.016	2.063	0.665	0.315	0.020	2.329	1.016	35.200
6.25		4.105	2.038	2.166	0.599	0.381	0.02002	2.361	0.992	36.030
9.375		4.098	2.061	2.296	0.516	0.464	0.02003	2.401	0.969	37.510
12.50		4.088	2.084	2.468	0.421	0.559	0.02004	2.455	0.948	39.830
15.63		4.075	2.108	2.696	0.307	0.673	0.02002	2.519	0.926	41.490
18.75		4.055	2.131	3.036	0.155	0.824	0.02008	2.663	0.962	49.810
19.34		4.051	2.136	3.111	0.121	0.859	0.02009	2.712	0.991	52.710
20.12	1	4.048	2.147	3.190	0.067	0.913	0.02009	2.835	1.103	60.140
20.51		4.052	2.158	3.181	0.038	0.942	0.02010	2.952	1.249	67.100
20.75		4.055	2.167	3.166	0.019	0.961	0.02010	3.031	1.367	72.020
20.85		4.063	2.180	3.087	0.0	0.980	0.01992	3.070	1.590	83.590
20.92	2	4.075	2.212	3.038	0.0	0.980	0.01992	2.842	2.678	155.80
21.07		4.069	2.231	3.188	0.0	0.980	0.01992	2.661	4.549	291.70
21.31		4.059	2.243	3.386	0.0	0.980	0.01992	2.631	7.867	530.40
21.46	3	4.048	2.248	3.590	0.0	0.980	0.01992	2.690	13.74	948.10
21.56		4.005	2.233	4.290	0.0	0.980	0.01992	3.624	75.05	4335.0
21.59		3.909	2.165	6.179	0.0	0.980	0.01992	6.392	597.6	21520
21.60	4	3.719	1.948	11.56	0.0	0.980	0.01992	9.553	2396.0	61000

Table 4-4: Same as Table 4-1 but for $M=3.750M_{\odot}$

t		$\log T_e$	$\log L/L_{\odot}$	$R/R_{\odot}$	X_c	Y_c	Z_c	T_c	$P_c/10^{17}$	D_c
10^7yrs		(^{0}K)						10^7K	dycm^{-2}	gcm^{-3}
0.0		4.165	2.287	2.191	0.730	0.250	0.020	2.397	0.860	26.280
1.172		4.162	2.300	2.248	0.696	0.284	0.020	2.421	0.858	28.310
3.125		4.158	2.322	2.349	0.637	0.343	0.02001	2.451	0.837	28.890
4.102		4.156	2.334	2.407	0.600	0.380	0.02002	2.462	0.823	28.100
6.250		4.149	2.361	2.566	0.516	0.464	0.02003	2.506	0.799	29.040
8.008		4.140	2.383	2.738	0.430	0.550	0.02004	2.554	0.781	30.460
9.375		4.132	2.403	2.911	0.357	0.623	0.02005	2.604	0.769	32.040
10.94		4.119	2.424	3.162	0.255	0.725	0.02007	2.685	0.768	35.280
12.50		4.103	2.447	3.499	0.125	0.855	0.02009	2.852	0.828	42.540
12.89	1	4.100	2.455	3.577	0.084	0.896	0.02009	2.939	0.886	46.040
13.28		4.106	2.473	3.558	0.038	0.942	0.02010	3.137	1.085	53.770
13.45		4.111	2.485	3.526	0.0	0.980	0.01959	3.043	1.273	67.130
13.50		4.120	2.502	3.448	0.0	0.980	0.01959	3.009	1.671	89.960
13.55	2	4.124	2.523	3.474	0.0	0.980	0.01959	2.904	2.453	138.90
13.60		4.122	2.534	3.552	0.0	0.980	0.01959	2.835	3.224	189.40
13.75		4.111	2.551	3.803	0.0	0.980	0.01959	2.770	5.923	368.40
13.87	3	4.092	2.559	4.185	0.0	0.980	0.01959	2.872	14.10	899.60
13.92		4.041	2.544	5.209	0.0	0.980	0.01959	4.166	91.13	4480.0
13.93		3.939	2.481	7.755	0.0	0.980	0.01959	6.943	553.4	17580
13.94	4	3.706	2.231	16.99	0.0	0.980	0.01959	9.695	1699.0	40300

Table 4-5: Same as Table 4-1 but for $M=4.375M_{\odot}$.

t		$\log T_e$	$\log L/L_{\odot}$	$R/R_{\odot}$	X_c	Y_c	Z_c	T_c	$P_c/10^{17}$	D_c
10^7yrs		(^{0}K)						10^7K	dycm^{-2}	gcm^{-3}
0.0		4.206	2.529	2.396	0.730	0.250	0.020	2.483	0.737	21.570
1.172		4.203	2.548	2.483	0.683	0.2976	0.02001	2.511	0.728	22.870
2.148		4.200	2.565	2.567	0.637	0.343	0.02001	2.534	0.715	23.170
3.125		4.196	2.582	2.662	0.590	0.390	0.02002	2.559	0.701	23.520
4.102		4.192	2.601	2.776	0.534	0.446	0.02003	2.590	0.688	24.080
5.078		4.186	2.620	2.914	0.474	0.506	0.02004	2.626	0.674	24.860
6.250		4.177	2.645	3.123	0.386	0.594	0.02005	2.673	0.655	24.990
8.008		4.156	2.684	3.595	0.221	0.758	0.02007	2.812	0.651	28.880
8.887		4.143	2.706	3.929	0.108	0.872	0.02009	2.980	0.708	34.520
9.082	1	4.141	2.713	3.992	0.079	0.901	0.02009	3.056	0.752	37.020
9.277		4.142	2.723	4.009	0.046	0.933	0.02010	3.175	0.842	40.970
9.375		4.149	2.734	3.937	0.0	0.980	0.02009	3.228	0.981	48.050
9.473		4.162	2.763	3.843	0.0	0.980	0.02009	3.052	1.614	85.460
9.497	2	4.163	2.774	3.866	0.0	0.980	0.02009	3.007	2.008	108.80
9.546		4.161	2.789	3.977	0.0	0.980	0.02009	2.939	2.930	164.80
9.619		4.153	2.804	4.192	0.0	0.980	0.02009	2.902	4.744	276.30
9.692	3	4.137	2.815	4.513	0.0	0.980	0.02009	2.962	10.09	602.10
9.729		4.084	2.807	5.782	0.0	0.980	0.02009	4.242	74.90	3500.0
9.743		3.900	2.698	11.90	0.0	0.980	0.02009	8.445	795.6	20380
9.744		3.806	2.613	16.65	0.0	0.980	0.02009	9.410	1136	26460
9.745	4	3.703	2.482	22.99	0.0	0.980	0.02009	9.962	1363	30140

Table 4-6: Same as Table 4-1 but for $M=5.0M_{\odot}$.

t		$\log T_e$	$\log L/L_{\odot}$	$R/R_{\odot}$	X_c	Y_c	Z_c	T_c	$P_c/10^{17}$	D_c
10^7yrs		(^{0}K)						10^7K	dycm^{-2}	gcm^{-3}
0.0		4.240	2.734	2.592	0.730	0.250	0.020	2.557	0.644	18.190
1.172		4.236	2.761	2.725	0.666	0.314	0.02001	2.600	0.633	19.770
2.148		4.232	2.786	2.853	0.603	0.376	0.02002	2.626	0.613	19.310
3.125		4.226	2.812	3.017	0.534	0.446	0.02003	2.666	0.596	19.730
4.102		4.218	2.840	3.233	0.447	0.533	0.02004	2.719	0.580	20.550
5.078		4.207	2.871	3.534	0.341	0.640	0.02006	2.795	0.567	22.060
6.250		4.186	2.909	4.073	0.179	0.801	0.02008	2.965	0.582	26.290
6.445		4.181	2.916	4.187	0.144	0.835	0.02008	3.021	0.598	27.790
6.836	1	4.177	2.936	4.373	0.068	0.912	0.02009	3.218	0.696	32.910
6.934		4.179	2.944	4.362	0.046	0.934	0.02010	3.323	0.767	35.490
7.056		4.185	2.958	4.313	0.0	0.980	0.020	3.454	0.909	41.040
7.080		4.191	2.966	4.238	0.0	0.980	0.020	3.359	1.048	49.160
7.098	2	4.200	2.986	4.162	0.0	0.980	0.020	3.295	1.519	73.790
7.123		4.196	3.008	4.352	0.0	0.980	0.020	3115	2.627	138.10
7.166		4.184	3.024	4.688	0.0	0.980	0.020	3.032	4.810	266.80
7.202	3	4.163	3.033	5.203	0.0	0.980	0.020	3.131	11.58	653.00
7.224		4.101	3.023	6.847	0.0	0.980	0.020	4.841	93.54	3776.0
7.231		3.939	2.939	13.12	0.0	0.980	0.020	8.429	602.7	14870
7.232		3.860	2.879	17.61	0.0	0.980	0.020	9.347	854.0	19240
7.233	4	3.732	2.743	27.15	0.0	0.980	0.020	10.06	1083	22850

each model gives the time elapsed since the ZAMS in units of 10^7 years. Following Section 2.2 we see that lower mass stars have longer M-S life time than massive stars (in agreement with other theoretical work see e. g. 23, 25, 26, 27). Table 4-7 shows the run of the main sequence life time on the mass of the models.

Table 4-7: M-S life time of the models as a function of mass.

M/M_Θ	$t(10^8$ yrs)
2.187	5.1950
2.50	3.6720
3.125	2.0850
3.750	1.3380
4.375	0.9375
5.000	0.7056

Column 2 and 3 of the tables give the logarithms of the effective temperature T_e and the relative luminosity L/L_Θ. Column 4 shows the relative radius R/R_Θ of the models and columns 5, 6, and 7 list the central hydrogen, helium, and heavy-element abundances. Finally columns 8, 9, and 10 present the central values of the temperature, pressure, and density of the models. Full details of different phase of evolution are given by Iben(23) (see also Section 4-1).

4-4 LOW MASS M-S MODELS

In the next two Sections we present a series of non-evolutionary models of 1.0, 0.9, 0.8, 0.7, 0.6, 0.5, 0.4, 0.3, 0.2, and 0.1 solar masses. The effect of molecules on the structure of these stars is investigated in the next section. In this section we calculate these models with the consideration of molecules in the opacities and equation of state. Input physics are as mentioned in Section 4-2. Models are calculated for both population types with α=1.0.

The most important parameters of the models are listed in Tables 4-8 to 4-11 for both population types. Table 4-8 presents some of the basic characteristics of the population I (0.770, 0.018) models and Table 4-9 those of the population II (0.783, 0.001) models. For each model in the tables its mass (solar unit), effective temperature, luminosity (s. u.), and radius (s. u.) are tabulated. Column 5, 6, and 7 of these tables represent the logarithm of the quantities. Unfortunately, 0.2 and 0.1 M_{Θ} main sequence models could not be obtained for population I models.

We will compare the present models with observational data in Section 4-5. The resultant main sequence positions of the models for both population types in the theoretical H-R diagram are shown in Fig.4-2. The break in these zero age lines at about $\log T_e$ = 3.62-3.65

Table 4-8: Theoretical zero age main sequence for population I models.

$M/M_\odot$	T_e	$L/L_\odot$	$R/R_\odot$	$\log T_e$	$\log L/L_\odot$	$\log R/R_\odot$
1.0	5128	0.749	1.106	3.710	-0.126	0.043
0.9	4820	0.443	0.962	3.683	-0.354	-0.017
0.8	4425	0.248	0.855	3.646	-0.605	-0.068
0.7	4109	0.134	0.729	3.614	-0.873	-0.137
0.6	3858	0.072	0.606	3.586	-1.143	-0.217
0.5	3584	0.0377	0.508	3.554	-1.424	-0.294
0.4	3350	0.0198	0.422	3.525	-1.702	-0.375
0.3	3215	0.0114	0.347	3.507	-1.944	-0.460

Table 4-9: Theoretical zero age main sequence for population II models.

1.0	6651	2.612	1.228	3.823	0.417	0.09
0.9	5821	1.591	1.251	3.765	0.202	0.097
0.8	5099	0.861	1.200	3.708	-0.065	0.079
0.7	4472	0.4179	1.087	3.650	-0.379	0.036
0.6	4130	0.180	0.836	3.616	-0.745	-0.078
0.5	3943	0.0759	0.596	3.596	-1.120	-0.225
0.4	4004	0.0405	0.422	3.603	-1.393	-0.375
0.3	3747	0.0192	0.3315	3.574	-1.717	-0.480
0.2	3479	0.0087	0.2586	3.541	-2.062	-0.587
0.1	3197	0.0027	0.1703	3.505	-2.572	-0.768

Fig. 4-2: Theoretical ZAMS models of pop. I with $0.3 \leq M/M_{\odot} \leq 1.0$ and (X, Z)=(0.770, 0.018) and pop. II with $0.1 \leq M/M_{\odot} \leq 1.0$ and (X, Z)=(0.783, 0.001). Squares show models of 0.2, 0.4, 0.6, $0.7M_{\odot}$ with (X, Z)=(0.749, 0.001).

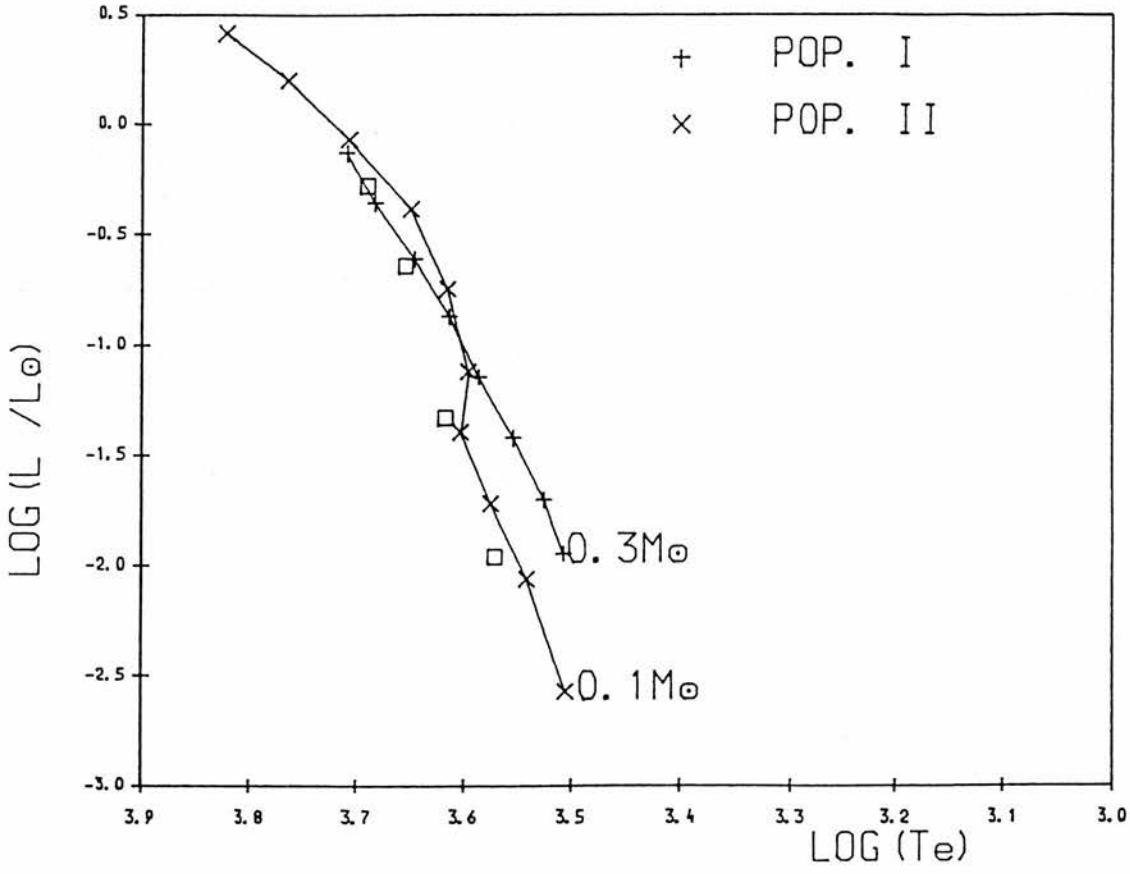

(hereafter T_b) is evident, although it is not too sharp for pop. I models. This break is affected by the non-ideal gas effects and molecular opacities. We will explain more about the existence of this break in the next section.

Fig. 4-2 shows that the slope of the zero age line is unaffected by composition changes, but there is a shift in the position of the line in the plane. According to Iben(23) in more massive models also the slope of the line is unaffected by composition changes. For a given mass, population II stars are more luminous and hotter than population I stars. At $0.3M_{\odot}$ the position of the models on the H-R diagram shifts by $\Delta \log T_e = 0.067$ horizontally (T direction) and $\Delta \log L/L_{\odot} = 0.227$ vertically (L direction) which is nearly the same as the separation of the Vandenberg's models (0.065 and 0.21) at this mass point when Z changes from 0.001 to 0.020. Vandenberg et al. (1983-30) have calculated main sequence models of 0.1 to $0.75M_{\odot}$ for 6 different composition using Alexander's opacities. They also (as in our models) concluded that the lowest Z stars should be hotter than the high Z stars of the same mass, implying that metal-poor low mass stars will be subluminous compared to their metal rich counterparts at the same effective temperature.

Above T_b metal-poor stars are slightly more luminous than the metal-rich ones at a given temperature. This may be, as mentioned by Iben(23), due to the bound-free absorption which will be more efficient in metal rich stars. But the separation of the lines is less than the other part. Iben and Renzini (1984-19) noted two main reasons why the luminosity of the stellar models is sensitive to the metal abundance parameter. Firstly, the so called middle-temperature opacities including bound-bound and bound-free transition involving occupied levels of elements (mainly C, N, O, Ne, etc.). The other is the efficiency of the CNO cycle which is proportional to the abundance of CNO elements and therefore to the value of Z.

Shown in Fig. 4-2, as open squares, are also the $0.2M_{\odot}$, $0.4M_{\odot}$, $0.6M_{\odot}$, and $0.7M_{\odot}$ models with (X,Y,Z)=(0.749,0.250,0.001). Comparing with the population II line, this show that decreasing X or increasing Y moves a star to the higher luminosity which is in agreement with the results of Vandenberg et al. (30) and Copeland et al. (21). In order to clarify the effect of changing X or Y on the main sequence loci of the models we have summarized the resultant data in a table:

	X=0.783 ,Y=0.216 ,Z=0.001				X=0.749 , Y=0.250 ,Z=0.001			
$M/M_\odot$	$R/R_\odot$	$\log T_e$	$\log L/L_\odot$	$T_c/10^7$	$R/R_\odot$	$\log T_e$	$\log L/L_\odot$	$T_c/10^7$
0.2	0.259	3.541	-2.062	0.6787	0.254	3.571	-1.262	0.7098
0.4	0.422	3.603	-1.393	0.8188	0.423	3.618	-1.330	0.8470
0.6	0.836	3.616	-0.745	1.013	0.789	3.655	-0.638	1.067
0.7	1.087	3.650	-0.379	1.151	1.019	3.690	-0.277	1.212

It is shown by the table that a reduction in X (or increase Y) results an increase in central temperature, effective temperature, and luminosity of the models.

There is good agreement between our pop. I models with theoretical works by G. D. Neece(1984-22) and Grossman et al.(1974-13), (X, Z)=(0.68, 0.03), which are shown in Fig. 4-3. Both Grossman et al. and Neece have calculated models with molecular opacities, as well as inclusion of electron degeneracy and Coulomb interaction in the equation of state. In the calculation by Neece more molecules (than Grossman) contribute to the opacities, but Grossman et al. have considered also the pressure ionization and dissociation in the equation of state. In our work a few more molecules are considered in the opacities. Fig. 4-4 shows the

Fig. 4-3: Comparison of pop. I, (X, Z)=(0.770, 0.018), models with theoretical works by Neece (1984) and Grossman et al. (1974), (X, Z)=(0.68, 0.03).

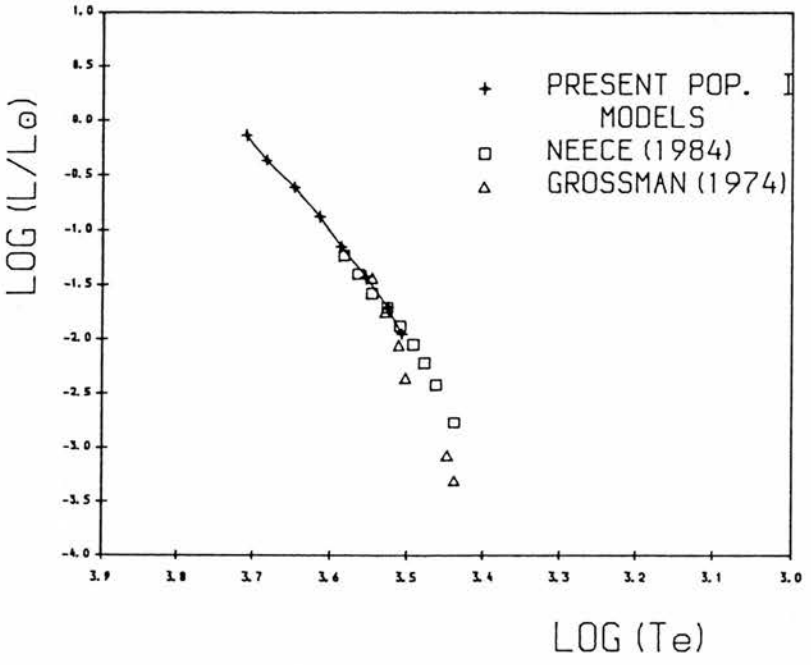

Fig. 4-4: Comparison of pop. II, (X, Z)=(0.783, 0.001), models with theoretical results by Vandenberg et al. (1983), (X, Z)=(0.799, 0.001).

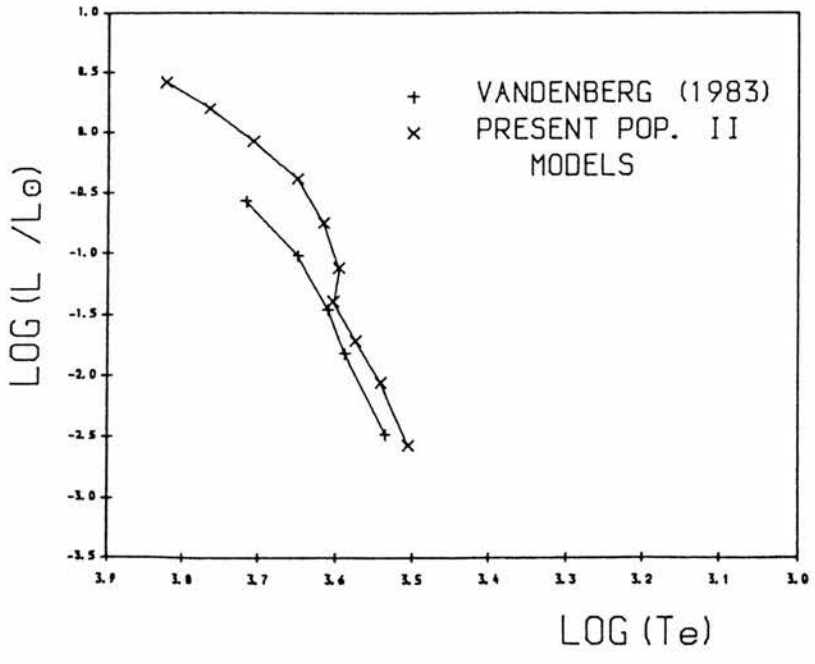

comparison of our pop. II (0.783, 0.001) models with the Vandenberg's models of (0.799, 0.001). Their equation of state includes H_2 dissociation and pressure ionization. Better agreement is below T_b where our models are cooler than Vandenberg's. At a given mass (and temperature) our models are more luminous, this may be partly due to the composition change in which a reduction in Y moves a star to lower luminosities. Other reason for disagreement are, of course, other input physics parameters including equation of state and opacity and even may be the radiative $T(\tau)$ relation in the atmospheres which, as mentioned by Grossman et al., has an effect on the position of the models (see next section).

Central quantities of the models for both two population types are tabulated in Tables 4-10 and 4-11. Column 1 of the tables gives the mass of the models in solar units. Columns 2, 3, and 4 indicate the central temperature ($T_c/10^7$), pressure ($P_c/10^{17}$), and density of the models. As expected, the central temperature (and pressure) decreases when mass decreases. Central density decreases with decreasing mass until the models become completely convective, and then increases strongly with decreasing mass. After this minimum, while the central density is increasing sharply, the magnitude of the

Table 4-10: Central quantities of the pop. I models. x_{co} and q_{co} show the radius and mass fraction at the bottom of the outer convective zone.

$M/M_\odot$	$T_c/10^7$	$P_c/10^{17}$	ρ_c	$\log\varepsilon_c$	x_{co}	q_{co}
1.0	1.297	1.282	76.94	2.661	0.8356	0.9977
0.9	1.194	1.125	73.73	2.263	0.770	0.9869
0.8	1.093	0.977	70.46	1.827	0.7293	0.9679
0.7	0.997	0.846	67.35	1.365	0.6904	0.9266
0.6	0.9111	0.736	64.62	0.900	0.6413	0.8433
0.5	0.8314	0.6414	62.20	0.417	0.586	0.7176
0.4	0.7629	0.5666	60.40	-0.043	0.5187	0.5390
0.3	0.7252	0.5470	61.24	-0.297	0.2877	0.1226

Table 4-11: Same as Table 4-10 but for pop. II models.

1.0	1.534	2.436	124.5	3.857	0.9993	1.000
0.9	1.426	2.195	121.6	3.536	0.9832	1.000
0.8	1.289	1.878	116.0	3.074	0.9301	1.000
0.7	1.151	1.561	109.1	2.525	0.8606	0.9993
0.6	1.013	1.262	101.2	1.878	0.7446	0.9826
0.5	0.894	1.021	93.8	1.213	0.6544	0.8950
0.4	0.8345	0.9101	90.08	0.839	0.5626	0.6546
0.3	0.7445	0.757	84.84	0.204	0.4522	0.3966
0.25	0.7197	0.734	85.67	0.039	0.287	0.1226
0.2	0.6787	0.7841	99.50	-0.120	completely convective	
0.1	0.5673	1.048	174.9	-0.542	completely convective	

decrease in the central temperature with mass diminishes. The run of the central density for pop. II type (because of the mass range) models is shown in Fig. 4-5 and 4-6. In Fig. 4-5 central density, after a minimum at around the complete convection (mass) point, increases sharply with decreasing mass. The slope of the decreasing line of the central temperature shown in Fig. 4-6, becomes much smaller after the minimum of the central density. Copeland et al. (21) concluded that the central density increases with decreasing mass as long as the CNO cycle produced the energy, and that the central density decreases with decreasing mass when the energy is generated by p-p reactions. Their results also show that in the complete convection mass region, central density again increases strongly with decreasing mass. This behaviour in the three mass regions was also reported by Iben(23).

Column 5 of the tables indicates that the energy production rate in the central zone decreases when mass (or when central temperature) decreases. Finally columns 6 and 7 of the tables show the radius and mass fraction at the bottom of the outer convective zone. The outer convection region develops as the mass decreases until at $0.2M_{\odot}$ the models (pop. II) become completely convective. This is in agreement with the result of Grossman et al. (13), which

Fig. 4-5: Central density versus mass in population II models with $0.1 \leq M/M_{\odot} \leq 1.0$.

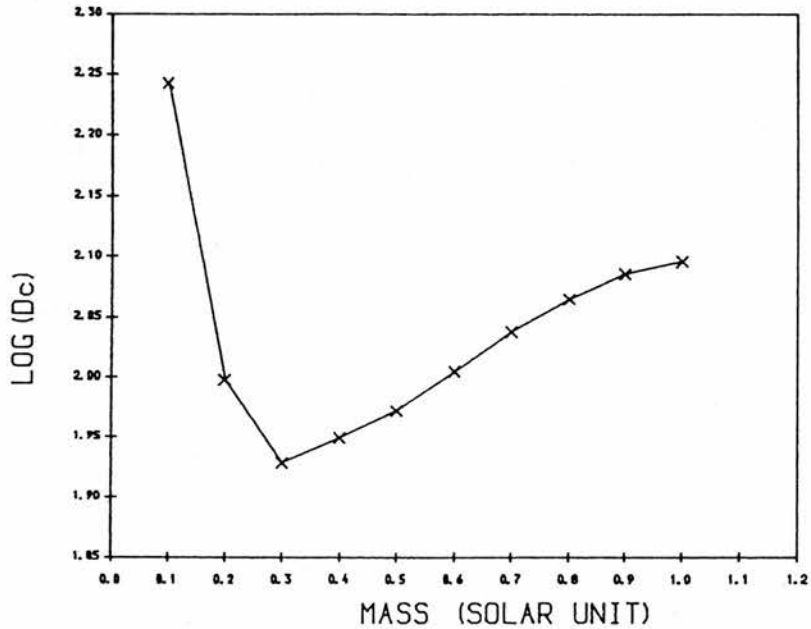

Fig. 4-6: Central temperature versus central density of the population II models with $0.1 \leq M/M_{\odot} \leq 1.0$.

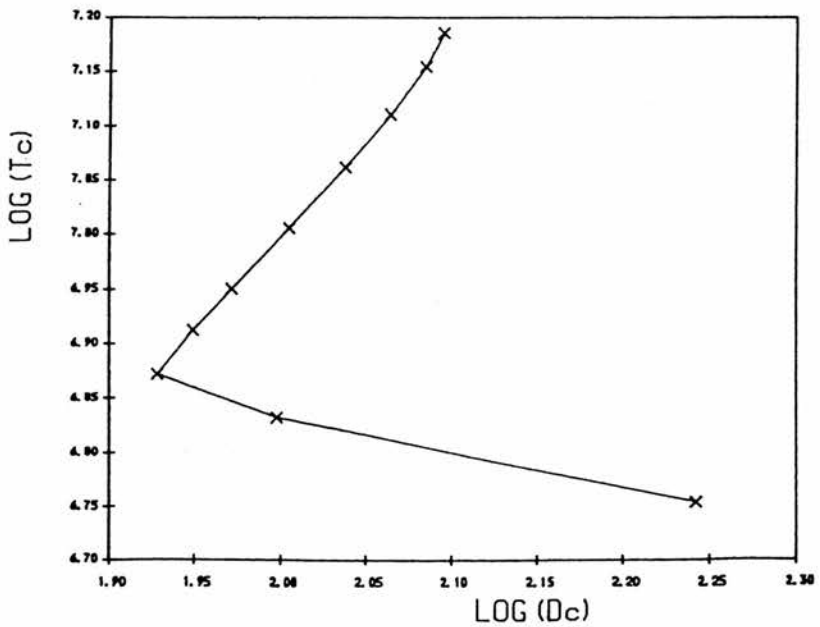

Neece (22) found $0.25M_{\odot}$ for this mass limit. Studies of the stellar structure show that, in general, stars with masses lower than $0.3\text{-}0.2M_{\odot}$ are found to be fully convective, while those of higher mass have a central radiative zone(see e. g. 22, 23, 13, 30). D'Antona (1985-14) noted that the first fully convective mass depends on the previous evolution (pre-main sequence) and on the consequent run of the equilibrium abundance of ^3He with time, in the central regions. A small convective core of 5-3 per cent of the total mass for masses above $0.4M_{\odot}$ has been reported by D'Antona(14) and Neece(22). Neece noted that this convective core has little effect on the overall structure of the star.

4-5 THE EFFECT OF MOLECULES ON THE STRUCTURE OF LOW MASS STARS

Copeland et al. (1970-21) have studied the effect of molecular hydrogen (H_2) on the structure of low mass stars. They have calculated zero age main sequence models for the mass range 0.25-2.50 $M_\odot$ with the equation of state with and without the inclusion of H_2 molecule. They found that inclusion of H_2 dissociation results in a break in the zero age line at $\log T_e = 3.64$ ($0.7M_\odot$) toward the higher temperatures. Their mass luminosity relation also shows this break at $M=0.5M_\odot$-$0.6M_\odot$ toward the higher luminosities. They concluded that the break in published computed zero age lines, as well as the break in the observed mass-luminosity relation at $M_{bol}=+7.5$ is due to the H_2 molecules. According to their results the break in zero age lines can easily be seen for lower Z composition.

Although Grossman et al. (1974-13) have calculated the models below $0.5M_\odot$, they estimated the mass corresponding to the break to be about $0.6M_\odot$. They noted that the improvements in constitutive physics such as electron degeneracy, Coulomb

interaction (in the eq. of st.), and electron screening (in the nuclear reactions) plus consideration of $^3He/H$ ratio and radiative $T(\tau)$ relation are also the basic reasons to produce a main sequence break at the observed mass, luminosity and effective temperature. They suggested that for effective temperatures less than 4000, T_b, molecular opacities sources also must be considered.Grossman et al. noted these effects as the reasons of the disagreement of the Copeland's results with observation in the spectral range below the break.

R. Sienkiewicz (1982-31) has calculated a set of models for $M \leq 0.3 M_\Theta$ using Cox-stewart $+H_2O$ opacities and Alexander opacities. Comparing his resultant models calculated by two kind of opacities, show that the models with Alexander have lower temperatures and luminosities at a given mass. This is because of the Alexander opacities which are, as mentioned by Vandenberg(30), larger at lower temperatures than the Cox-stewart opacities.

Neece(1984-22) determined the sensitivity of the $0.35 M_\Theta$ model to the various parameters and constitutive relations such as mixing length,^3He abundance, molecular opacities, and particle interaction. The result was that the effects of (ignoring or not) molecular

opacities and particle interaction are much more than the others. Fig. 3 of his paper shows a considerable change in the position of the model on the H-R diagram, firstly due to ignoring molecular opacities and then without inclusion of particle interaction in the equation of state.

When we started to make main sequence models, we concentrated our work on the effect of molecular opacities on the structure of low mass stars. We made models with (X, Z)=(0.730, 0.020) as population I and (0.749 ,0.001) as population II for the mass range 0.1 to 1.0 solar mass and α=1.0. The models were calculated with and without consideration of molecular opacities using simple equation of state (no molecule formation). The resultant effective temperature, luminosity, radius, and central temperature of the pop. I and pop. II models are tabulated in Tables 4-12 and 4-13. Column 1 of the tables gives the mass of the models in solar unit. Columns 2, 3, 4, and 5 indicate the properties of the models when molecular opacities are included while columns 6, 7, 8, and 9 show those quantities when molecular opacities are ignored.

Comparing these data in Fig. 4-7 indicates the general result of lowering luminosity and effective temperature by increasing opacity (inclusion of molecules) in the both population types

Table 4-12: The effect of molecular opacities on the theoretical main sequence population I models using simple equation of state.

	With molecular opacities				Without molecular opacities			
$M/M_\odot$	$\log T_e$	$\log L/L_\odot$	$\log R/R_\odot$	$T_c/10^7$	$\log T_e$	$\log L/L_\odot$	$\log R/R_\odot$	$T_c/10^7$
1.0	3.699	-0.048	0.105	1.358	3.714	-0.048	0.074	1.358
0.9	3.656	-0.269	0.081	1.258	3.687	-0.268	0.019	1.259
0.8	3.599	-0.527	0.064	1.148	3.676	-0.513	-0.090	1.153
0.7	3.565	-0.820	-0.013	1.037	3.675	-0.738	-0.193	1.067
0.6	3.521	-1.149	-0.090	0.928	3.674	-0.931	-0.287	0.999
0.5	3.493	-1.490	-0.205	0.830	3.665	-1.123	-0.363	0.940
0.4	3.474	-1.807	-0.326	0.750	3.645	-1.336	-0.432	0.887
0.3	3.444	-2.141	-0.433	0.680	3.623	-1.572	-0.505	0.821
0.2	3.389	-2.572	-0.538	0.604	3.600	-1.874	-0.610	0.732
0.1	3.304	-3.252	-0.708	0.485	3.562	-2.391	-0.793	0.608

Table 4-13: Same as Table 4-12 but for pop. II models.

1.0	3.856	0.537	0.0824	1.657	3.856	0.537	0.082	1.657
0.9	3.798	0.315	0.0888	1.516	3.798	0.315	0.088	1.516
0.8	3.731	0.055	0.0916	1.371	3.734	0.055	0.086	1.371
0.7	3.667	-0.254	0.0663	1.223	3.683	-0.253	0.033	1.223
0.6	3.606	-0.621	0.0158	1.074	3.646	-0.616	-0.074	1.076
0.5	3.556	-1.055	-0.1124	0.9269	3.638	-0.983	-0.242	0.949
0.4	3.524	-1.504	-0.2733	0.8013	3.638	-1.276	-0.387	0.863
0.3	3.505	-1.893	-0.4306	0.7105	3.629	-1.540	-0.5016	0.8003
0.2	3.465	-2.318	-0.5622	0.6362	3.607	-1.850	-0.6126	0.7331
0.1	3.372	-3.022	-0.7282	0.5115	3.571	-2.359	-0.795	0.6096

Fig. 4-7: The effect of molecular opacity on the structure of low mass models with $0.1 \leq M/M_{\odot} \leq 1.0$ and using simple equation of state. Models are shown as: +, population I without molecular opacity; ×, pop. II without molecular opacity; Δ, pop. I with molecular opacity; and □, pop. II with molecular opacity.

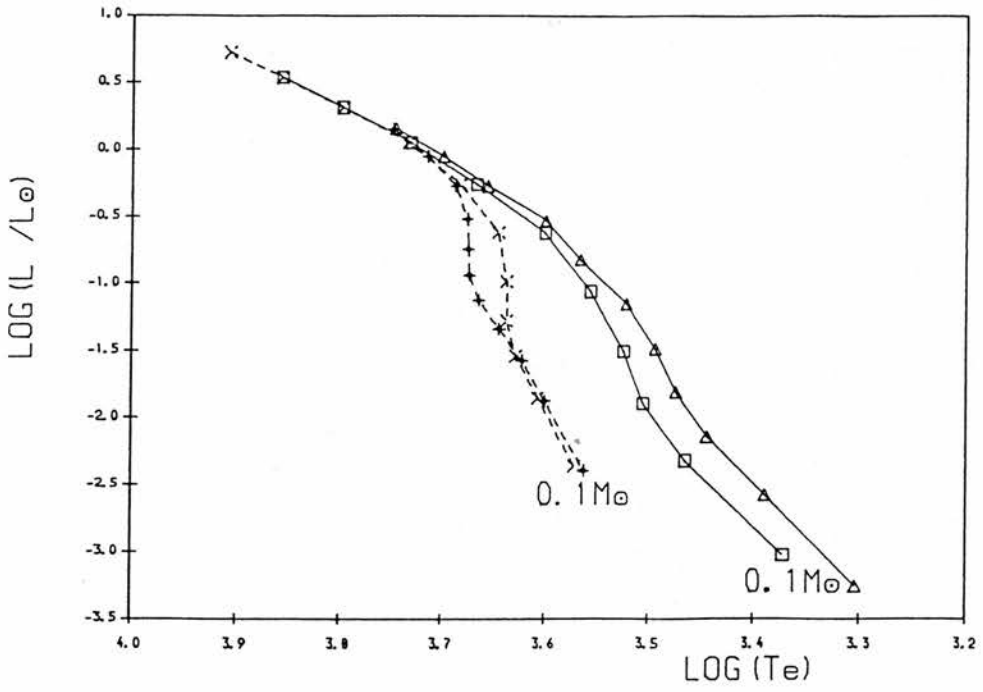

models (see also 31, 22, 14). Full lines indicate the main sequence models with molecular opacities, where dashed lines those ignoring molecules. The effect of molecular opacities starts at $\log T_e = 3.68$ where the zero age lines turn toward the higher temperature due to ignoring molecules. For a given mass and composition, ignoring molecular opacities moves the models toward the higher luminosity and effective temperature. The lowest mass models without inclusion of molecular opacities are nearly insensitive to the composition change, while the lines with inclusion of molecules are well separated in both direction. This, in fact, shows the effect of molecules of the heavy elements. Table 4-12 and 4-13 show that the exclusion of molecular opacities also causes a reduction in radius and an increase in the central temperature of the models which is also concluded by Neece (22).

The effect of ignoring molecules in the equation of state is presented by Tables 4-14 and 4-15 and illustrated in Fig. 4-8. we have calculated the models presented in the last section when no molecules were considered in the equation of state. Tables show the properties of the models with molecular opacities, but with and without considering formation of molecules in the equation of state. Data in the tables are concentrated on the effective temperature,

Table 4-14: The effect of molecular equation of state on the theoretical main sequence Population I models. molecular opacities are considered.

	Molecular equation of state				Simple equation of state			
$M/M_\odot$	$\log T_e$	$\log L/L_\odot$	$\log R/R_\odot$	$T_c/10^7$	$\log T_e$	$\log L/L_\odot$	$\log R/R_\odot$	$T_c/10^7$
1.0	3.710	-0.126	0.043	1.297	3.677	-0.135	0.105	1.288
0.9	3.683	-0.354	-0.0166	1.194	3.641	-0.358	0.065	1.193
0.8	3.646	-0.605	-0.068	1.093	3.597	-0.618	0.023	1.088
0.7	3.614	-0.873	-0.137	0.9973	3.574	-0.903	-0.073	0.9871
0.6	3.586	-1.143	-0.217	0.9111	3.572	-1.166	-0.199	0.9041
0.5	3.554	-1.424	-0.294	0.8314	3.547	-1.439	-0.287	0.8273
0.4	3.525	-1.702	-0.375	0.7629	3.501	-1.768	-0.362	0.7462
0.3	3.507	-1.944	-0.460	0.7252	3.456	-2.115	-0.442	0.676

Table 4-15: Same as 4-14 but for Population II models.

1.0	3.823	0.417	0.09	1.534	3.827	0.446	0.095	1.558
0.9	3.765	0.202	0.097	1.426	3.764	0.199	0.0989	1.420
0.8	3.708	-0.065	0.079	1.289	3.703	-0.067	0.086	1.285
0.7	3.650	-0.379	0.036	1.151	3.642	-0.381	0.0511	1.147
0.6	3.616	-0.745	-0.078	1.013	3.589	-0.752	-0.027	1.008
0.5	3.596	-1.120	-0.225	0.8936	3.569	-1.154	-0.188	0.8812
0.4	3.603	-1.393	-0.375	0.8188	3.556	-1.506	-0.338	0.787
0.3	3.574	-1.717	-0.480	0.7445	3.536	-1.832	-0.461	0.714
0.2	3.541	-2.062	-0.587	0.6787	3.486	-2.249	-0.569	0.643
0.1	3.505	-2.572	-0.768	0.5673	3.390	-2.957	-0.733	0.5114

Fig. 4-8: The effect of molecular equation of state on the structure of low mass models with $0.1 \leq M/M_{\odot} \leq 1.0$. Models are shown as: +, population I without molecules; ×, pop. II without molecules; □, pop. II with molecules; and Δ, pop. I with molecules. Molecular opacities are included.

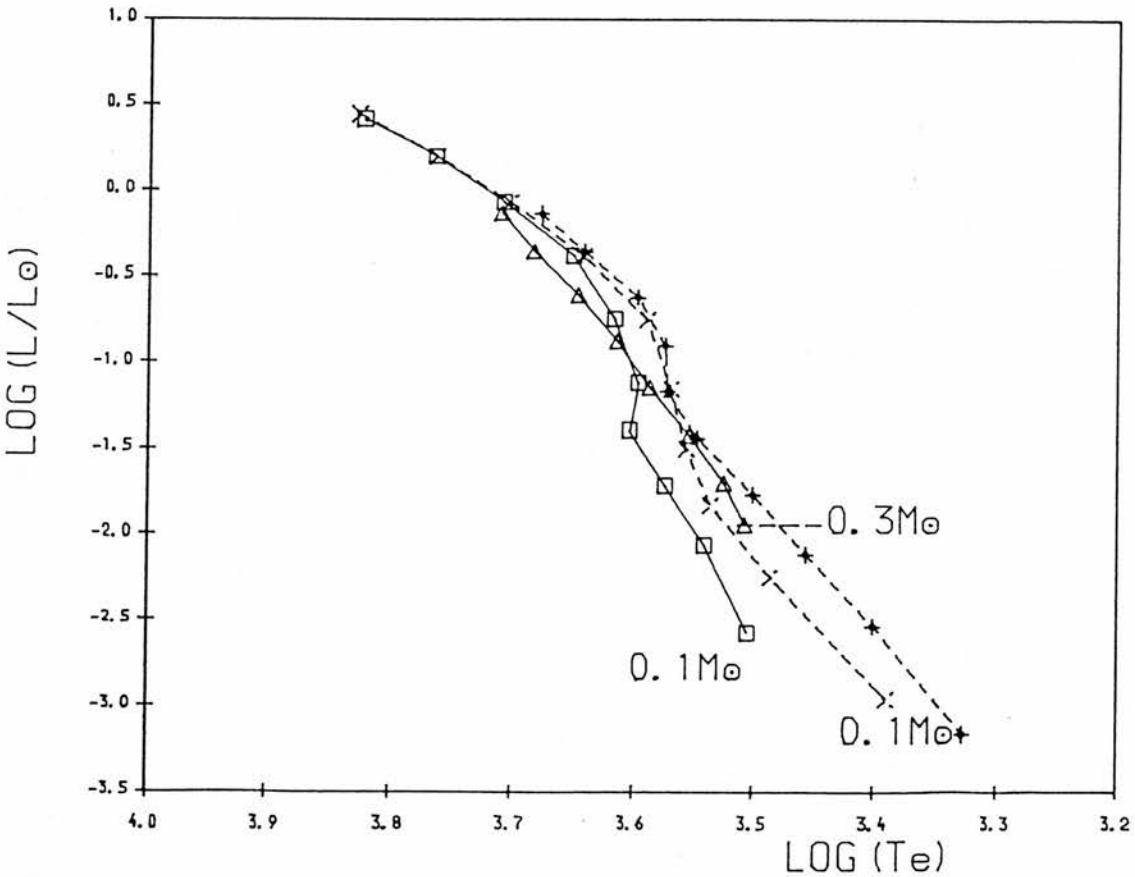

luminosity, radius, and central temperature of the models.

Fig. 4-8 shows the effect of the molecular equation of state for both population types presented in the tables. Full lines indicate the positions of models with molecule formation in the equation of state and dashed lines those ignoring molecules. The result of the exclusion of molecules is to move the models toward the lower luminosities and effective temperatures. This is in agreement with the results of Copeland et al. (21). In a given population type (composition) the separation between models, particularly in the luminosity direction, is more considerable in the low mass stars than in massive ones. Exclusion of molecules in the equation of state also results in a reduction in the central temperature but an increase in the radius of the models. Copeland et al. (21) noted that the change in the position of the models is due to the change in the pressure and temperature gradient. The exclusion of molecule formation, however, change the position of the models in the H-R diagram and so is effective on the known break in the zero age line and on the accuracy of the models.

In addition to the molecules other input physics including all other nonideal gas effects are also effective in the accuracy of the models. Models shown in Fig. 4-2 were calculated including

molecules in opacities and equation of state. The break toward the higher temperatures is evident in the curves, although for population I it is not too sharp. Fig. 4-7 shows the models without inclusion of molecules in the equation of state and Fig. 4-8 those calculated with molecular opacities. In all of the curves the break at $\log T_e$=3.60-3.68 is evident but the point at which it occurs and the magnitude of the break depend on the particular stellar parameters and composition. The results of Copeland et al. (21) also show the dependence of this point to the composition of the models. The break in all of the curves shows that some other parameters, as mentioned by Grossman et al. (13) and by Neece (22), also must contribute to the break. As the result by Neece shows, a considerable change in the position of the model is due to ignoring particle interactions in the equation of state. So, although the most important factors in the accuracy of the models may be molecules, low mass models also are sensitive to the other factors, including nonideal effects.

The role of the mixing length to scale height ratio, α, in the structure of low mass stars has been investigated by some authors. Copeland et al.(21) found that the luminosity of the lower mass models is sensitive to the mixing length. Cox et al.(1981-32) suggested

that the assumed value of the mixing length parameter in the models of $M \leq 0.3 M_{\odot}$ (pop. I) should be smaller than the conventional values of 1.0 or 2.0. Although the $0.35 M_{\odot}$ (and high Z) model of Neece is relatively insensitive to the α, there is a small shift toward the higher temperatures when α change from 1.0 to 2.0. We also recalculate population II (low Z) model of $0.4 M_{\odot}$, which shows an irregular behaviour (making a maximum of T_e) as it is evident in Fig. 4-2, for α=2.0, 0.6, 0.5, 0.4, 0.3, 0.2, and 0.1. Other input physics were as in the last Section. The most convenient value was 0.2 which shifts the model by $\Delta \log T_e = 0.065$ toward the lower temperature (and luminosity) to fit this model to the observation. We then calculated other masses (starting from $0.1 M_{\odot}$) with this value of α until $0.6 M_{\odot}$, which for higher masses we had difficulty with convergence in the models. The best fit was for $M \leq 0.5 M_{\odot}$ where the models were completely fitted to the observation (see Fig. 4-9,b in the next section). The resultant models along with the corresponding models of α=1.0, taken from Table 4-9, are given below:

	α=0.2			α=1.0		
$M/M_\odot$	$\log R/R_\odot$	$\log T_e$	$\log L/L_\odot$	$\log R/R_\odot$	$\log T_e$	$\log L/L_\odot$
0.1	-0.760	3.491	-2.626	-0.768	3.505	-2.572
0.2	-0.576	3.510	-2.164	-0.587	3.541	-2.062
0.3	-0.444	3.508	-1.908	-0.480	3.574	-1.717
0.4	-0.319	3.538	-1.541	-0.375	3.603	-1.393
0.5	-0.155	3.549	-1.168	-0.225	3.596	-1.120
0.6	-0.0046	3.578	-0.751	-0.0777	3.616	-0.745

This table and the Fig.(4-9,b) along with a few models which we have made for α=1.5 and 2.0 (see also following tables) show that increasing mixing length reduces the radius of the models and increases effective temperature, central temperature, and luminosity (even for $M \leq 0.3M_\odot$ mentioned by Cox et al.). The change in the luminosity (and central temperature) is smaller for higher masses such that the luminosity of the $0.8M_\odot$ was insensitive when α changed from 1.0 to 1.5. The above table also show $\Delta \log L/L_\odot = 0.102$ for $0.2M_\odot$ while $\Delta \log L/L_\odot = 0.006$ for $0.6M_\odot$(see also Fig. 4-9,b). Copeland et al.(21) also noted that the luminosity of the low mass models is more sensitive to the mixing length than the massive ones. This may be due to the thick outer layer convection

zone or the complete convection in these models.

The effect of molecular opacities and mixing length on the evolutionary models are presented in Tables 4-16 through 4-20. The evolutionary models of $M=1.0M_{\odot}$ with $\alpha=0.5$, 1.0, and 2.0 and population I composition are calculated using molecular equation of state with and without molecular opacities. Column 1 of the tables gives the age and column 2, 3, and 4 indicate the surface properties of the models. Central structure including temperature, density, and composition are presented in columns 5, 6, 7, 8, and 9. The best result is given by $\alpha=2.0$ which gives $R\approx1.0R_{\odot}$ and $L\approx1.0L_{\odot}$ after $t=3.7E10^{9}$ and $3.8E10^{9}$ years when molecular opacities are and are not considered (Tables 4-17 and 4-20).

The effect of molecules and mixing length are the same as in main sequence models, mentioned above. For a given opacity and age the result of increasing mixing length is a reduction in the radius and increase in luminosity and effective temperature of the models. Ignoring molecular opacities, at a given α and same age, also reduce radius and increase luminosity and temperature of the

Table 4-16: Evolution of $1.0M_{\odot}$ star of pop. I, (X,Z)=(0.770, 0.018), with α=1.0. Molecular equation of state and molecular opacity are considered.

t	$R/R_{\odot}$	$L/L_{\odot}$	T_e	T_c	ρ_c	X_c	Y_c	Z_c
10^8yrs			^{0}K	$10^7\,^0$K	gcm^{-3}			
0.0	1.221	0.7485	4881	1.297	76.95	0.770	0.212	0.0180
1.0	1.260	0.7528	4812	1.300	77.71	0.7632	0.2188	0.0180
2.0	1.240	0.7575	4857	1.303	78.49	0.7564	0.2256	0.0180
3.0	1.191	0.7623	4964	1.306	79.29	0.7496	0.2324	0.0180
4.0	1.139	0.7674	5084	1.309	80.11	0.7427	0.2393	0.0180
5.0	1.098	0.7730	5188	1.312	80.96	0.7359	0.2461	0.0180
6.0	1.073	0.7786	5258	1.316	81.81	0.7290	0.2530	0.01801
7.0	1.063	0.7839	5292	1.319	82.69	0.7221	0.2599	0.01801
9.0	1.062	0.7942	5311	1.326	84.49	0.7082	0.2738	0.01801
13.0	1.072	0.8151	5321	1.340	88.31	0.6804	0.3016	0.01801
17.0	1.083	0.8372	5329	1.354	92.48	0.6522	0.3297	0.01802
21.0	1.094	0.8607	5338	1.369	97.05	0.6235	0.3581	0.01802
25.0	1.106	0.8856	5348	1.385	102.1	0.5952	0.3868	0.01802
29.0	1.119	0.9121	5357	1.402	107.6	0.5662	0.9158	0.01803
33.0	1.131	0.9404	5369	1.420	113.7	0.5368	0.4451	0.01803
39.0	1.145	0.9704	5378	1.439	120.5	0.5071	0.4748	0.01803
41.0	1.163	1.006	5384	1.465	128.4	0.4770	0.5050	0.01804

Table 4-17: Evolution of $1.0M_{\odot}$ star of pop. I, (X,Z)=(0.770, 0.018), with α=2.0. Molecular equation of state and molecular opacities are considered.

t	$R/R_{\odot}$	$L/L_{\odot}$	T_e	T_c	ρ_c	X_c	Y_c	Z_c
10^8yrs			^{0}K	10^7 ^{0}K	gcm^{-3}			
0.0	1.154	0.7488	5030	1.297	76.95	0.770	0.212	0.018
1.0	1.122	0.7535	5099	1.300	77.71	0.7632	0.2188	0.018
3.0	1.067	0.7640	5247	1.306	79.31	0.7496	0.2324	0.018
5.0	1.009	0.7766	5418	1.313	80.98	0.7359	0.2461	0.018
7.0	0.965	0.7968	5566	1.321	82.75	0.7220	0.2600	0.01801
9.0	0.9434	0.8042	5653	1.329	84.58	0.7081	0.2739	0.01801
13.0	0.9436	0.8263	5691	1.343	88.45	0.6800	0.3020	0.01801
17.0	0.9512	0.8487	5706	1.357	92.68	0.6516	0.3304	0.01802
21.0	0.9618	0.8722	5713	1.372	97.30	0.6229	0.3591	0.01802
25.0	0.9722	0.8971	57.23	1.388	102.4	0.5939	0.3881	0.01802
29.0	0.9823	0.9239	5735	1.405	108.0	0.5646	0.4174	0.01803
33.0	0.9924	0.9524	5749	1.424	114.2	0.5350	0.4470	0.01803
37.0	1.002	0.9830	5767	1.443	121.1	0.5050	0.4770	0.01803
41.0	1.016	1.019	5778	1.469	129.1	0.4745	0.5074	0.01804
45.0	1.029	1.054	5790	1.492	137.9	0.4428	0.5331	0.01804
49.0	1.043	1.090	5802	1.517	147.8	0.4104	0.5716	0.01805
53.0	1.058	1.132	5815	1.545	159.0	0.3763	0.6051	0.01805
57.0	1.072	1.174	5827	1.575	171.8	0.3417	0.6402	0.01806

Table 4-18: Evolution of $1.0M_{\odot}$ star of pop. I, (X,Z)=(0.770, 0.018), with Molecular equation of state and without molecular opacity, α=0.5.

t	$R/R_{\odot}$	$L/L_{\odot}$	T_e	T_c	ρ_c	X_c	Y_c	Z_c
10^8yrs			^{0}K	$10^7\,^0$K	gcm^{-3}			
0.0	1.190	0.7486	4944	1.297	76.95	0.770	0.212	0.018
2.0	1.204	0.7576	4929	1.303	78.49	0.7564	0.2256	0.018
6.0	1.207	0.7766	4953	1.315	81.78	0.7291	0.2529	0.01801
10.0	1.196	0.7967	5008	1.328	85.35	0.7015	0.2805	0.01801
14.0	1.184	0.8180	5067	1.342	89.24	0.6737	0.3083	0.01801
18.0	1.175	0.8407	5121	1.357	93.49	0.6456	0.3364	0.01802
22.0	1.178	0.8646	5152	1.372	98.15	0.6172	0.3648	0.01802
26.0	1.185	0.8899	5172	1.388	103.3	0.5885	0.3935	0.01802
30.0	1.200	0.9168	5179	1.406	108.9	0.5595	0.4225	0.01803
38.0	1.234	0.9759	5188	1.443	122.2	0.5004	0.4816	0.01803
42.0	1.255	1.012	5190	1.470	130.2	0.4702	0.5118	0.01804
46.0	1.275	1.046	5194	1.492	139.1	0.4387	0.5432	0.01804
50.0	1.295	1.083	5197	1.517	149.1	0.4065	0.5754	0.01805
54.0	1.318	1.125	5202	1.545	160.3	0.3733	0.6087	0.01805
58.0	1.341	1.166	5204	1.575	173.1	0.3384	0.6436	0.01806

Table 4-19: Evolution of $1.0M_{\odot}$ star of pop. I, (X,Z)=(0.770, 0.018), with molecular equation of state and without molecular opacity, α=1.0.

t	$R/R_{\odot}$	$L/L_{\odot}$	T_e	T_c	ρ_c	X_c	Y_c	Z_c
10^8yrs			^{0}K	$10^7\,^0$K	gcm^{-3}			
0.0	1.117	0.7491	5103	1.297	76.96	0.770	0.21	0.018
1.0	1.083	0.7542	5192	1.300	77.72	0.7632	0.2188	0.018
3.0	1.056	0.7645	5277	1.306	79.31	0.7496	0.2324	0.018
7.0	1.029	0.7853	5381	1.320	82.69	0.7221	0.2599	0.01801
11.0	1.021	0.8067	5439	1.333	86.36	0.6944	0.2876	0.01801
15.0	1.024	0.8285	5466	1.347	90.36	0.6663	0.3156	0.01801
19.0	1.034	0.8514	5477	1.362	94.73	0.6380	0.3440	0.01802
23.0	1.046	0.8754	5483	1.378	99.53	0.6094	0.3726	0.01802
27.0	1.059	0.9010	5488	1.394	104.8	0.5805	0.4014	0.01802
31.0	1.073	0.9283	5494	1.411	110.6	0.5513	0.4306	0.01803
35.0	1.087	0.9574	5501	1.430	117.1	0.5218	0.4602	0.01803
39.0	1.101	0.9884	5508	1.450	124.3	0.4918	0.4902	0.01804
43.0	1.120	1.025	5513	1.477	132.6	0.4614	0.5206	0.01804
47.0	1.137	1.060	5518	1.500	141.8	0.4296	0.5523	0.01804
51.0	1.154	1.098	5524	1.526	152.2	0.3970	0.5849	0.01805
55.0	1.173	1.140	5531	1.554	163.9	0.3633	0.6187	0.01805

Table 4-20: Evolution of $1.0M_{\odot}$ star of pop. I, (X,Z)=(0.770, 0.018), with Molecular equation of state and without molecular opacity, α=2.0.

t	$R/R_{\odot}$	$L/L_{\odot}$	T_e	T_c	ρ_c	X_c	Y_c	Z_c
10^8yrs			^{0}K	10^7 ^{0}K	gcm^{-3}			
0.0	1.0660	0.7502	5227	1.297	76.97	0.770	0.212	0.01800
1.0	0.9993	0.7581	5412	1.301	77.75	0.7632	0.2188	0.01800
2.0	0.9557	0.7670	5550	1.305	78.57	0.7563	0.2257	0.01800
3.0	0.9231	0.7766	5665	1.310	79.42	0.7493	0.2323	0.01800
4.0	0.9107	0.7837	5717	1.314	80.27	0.7425	0.2395	0.01800
6.0	0.9101	0.7942	5737	1.320	81.99	0.7286	0.2534	0.01801
10.0	0.9190	0.8141	5745	1.333	85.63	0.7005	0.2815	0.01801
14.0	0.9294	0.8351	5749	1.347	89.60	0.6722	0.3098	0.01801
18.0	0.9396	0.8575	5756	1.362	93.94	0.6436	0.3384	0.01802
22.0	0.9492	0.8815	5766	1.377	98.70	0.6148	0.3672	0.01802
26.0	0.9592	0.9070	5777	1.394	103.9	0.5857	0.3963	0.01802
30.0	0.9699	0.9342	5788	1.411	109.7	0.5562	0.4257	0.01803
34.0	0.9812	0.9632	5798	1.430	116.1	0.5264	0.4555	0.01803
38.0	0.9933	0.9940	5809	1.449	123.3	0.4963	0.4857	0.01804
42.0	1.0090	1.030	5816	1.476	131.5	0.4656	0.5164	0.01804
46.0	1.0230	1.066	5825	1.499	140.6	0.4336	0.5483	0.01804

models. In both cases the effect on the luminosity is not relatively considerable and central quantities are insensitive which may be due to the high central temperature and thin outer layer convective zone.

We must conclude by saying that ignoring molecules in the opacities and equation of state in low mass stars shift their position in the H-R diagram in opposite directions. Low temperature opacities and nonideal gas effects as well as some other parameters including mixing length determine the slope of the zero age line in the low mass stars . This slope is, of course, different with that of the more massive stars. In particular, considering molecules in the calculation, the change in the slope occurs at $\log T_e = 3.62\text{-}3.65$ depending on the composition and input physics. Our mass-luminosity relation (Fig. 4-11) also shows this break at a mass between 0.4 and $0.5 M_\odot$. We finally believe that the structure of low mass stars is sensitive to the low temperature opacities and nonideal gas effects.

4-6 COMPARISON WITH OBSERVATIONS

We have compared our models with observation in temperature-luminosity, mass-luminosity, and radius-luminosity

diagrams. Fig. 4-9,a compares our "theoretical" models (with α=1.0) with observation in the H-R diagram. The observational data in this diagram comes from a compilation of, spectrographic observation of, eclipsing binaries by Popper(1980-33) and an infrared photometry of very low mass dwarfs by Reid & Gilmore (1984-8). The models are shown as in Fig. 4-2, open squares show the observational data from Popper, and open triangles those of Reid & Gilmore.

The agreement between theory and observation for population I appears to be quite good for the most part of the diagram. Fig. 4-10 illustrates the theoretical and observational radius-luminosity diagram with Reid's observed data and Fig. 4-11 those of mass-luminosity with Popper's data. There is a good agreement for, say, all parts of the M-L diagram in population I. It seems the slight deviation in this type above T_b (temperature of the break) must be due to the discrepancy in temperature or radius. In population II models two deviations around $\log L/L_{\odot}$=-1.4 and -0.35 occur which in the first one the models are too hot and, relative to the Reid's data, more luminous. The effect of the mixing length parameter (α) to fit these models to the observation has been discussed in the last section and illustrated in Fig. 4-9,b. As it

Fig. 4-9,a: Comparison of the models with observational data by Popper (1980) and Reid & Gilmore(1984).

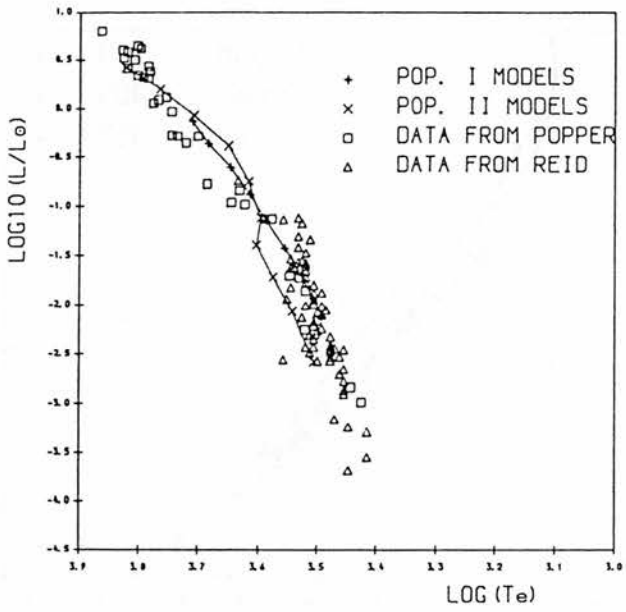

Fig. 4-9,b: Comparison of population II models with observational data. Models with $M \leq 0.5$ and $\alpha=0.2$ are quite in agreement with observation.

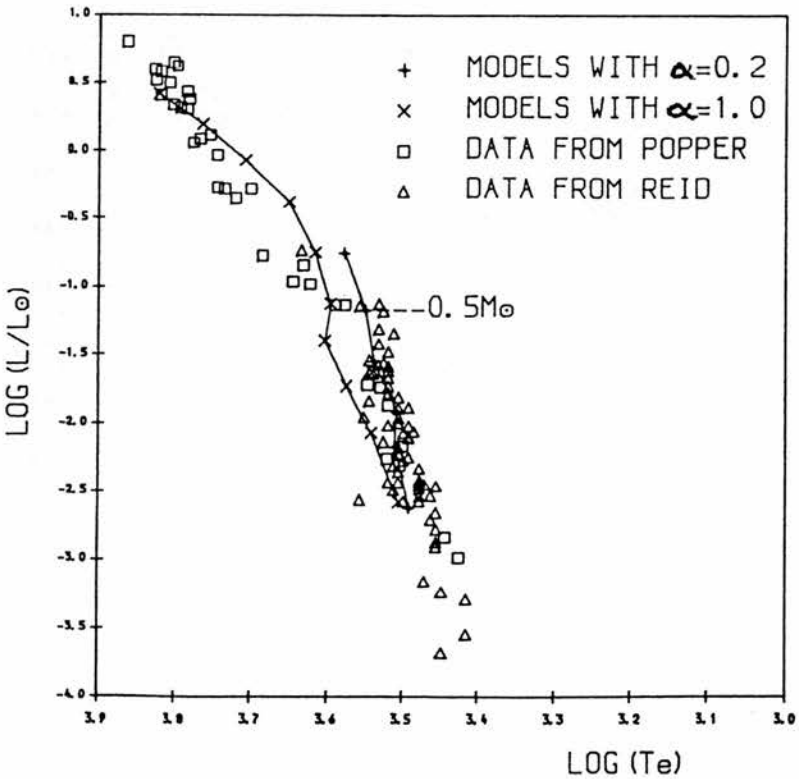

Fig. 4-10: Comparison of the models with observational data by Reid & Gilmore (1984) in Radius-Luminosity diagram.

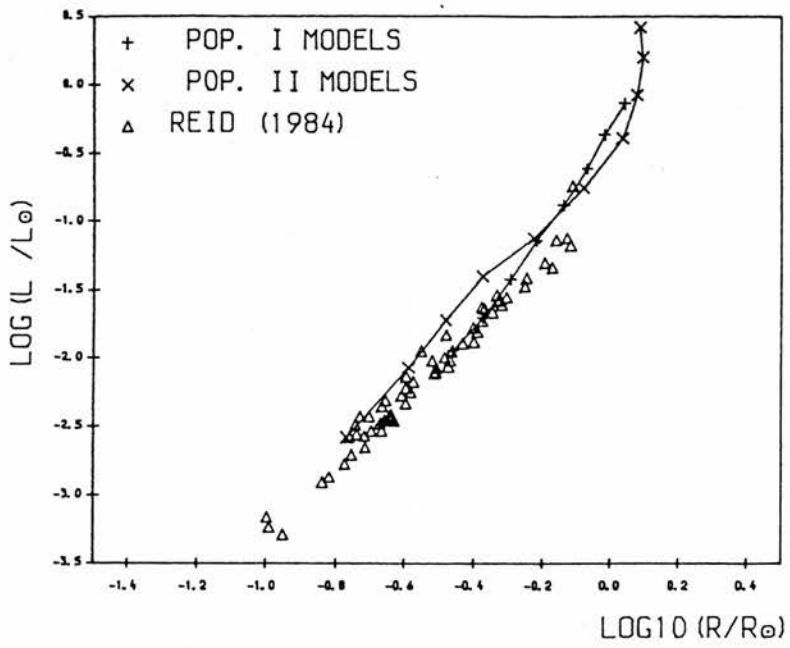

Fig. 4-11: Comparison of the models with data of Popper(1980) in Mass-Luminosity diagram.

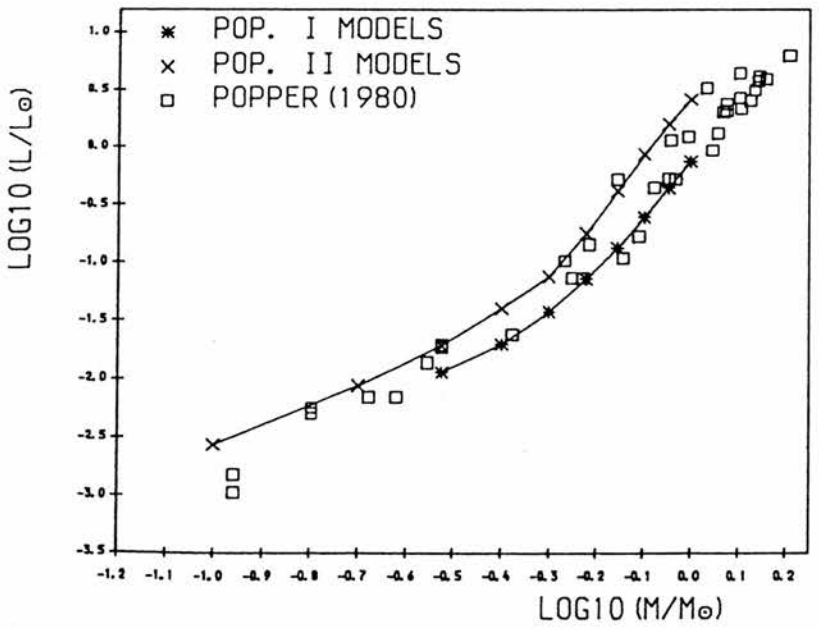

is evident from the figure population II models of $M \leq 0.5M_{\odot}$ with $\alpha=0.2$ are completely in agreement with observations.

The deviation, in population II and $\alpha=1.0$, around $\log L/L_{\odot}=-1.4$ ($0.4M_{\odot}$) is also evident in Fig. 4-10. It seems the discrepancy is in both luminosity and effective temperature relative to the Reid's data. In both Figures 4-9,a and 4-10, there is better agreement with observation for lower masses. Although there is not a sharp disagreement at $\log L/L_{\odot}=-1.4$ in mass-luminosity diagram(4-11), the lowest mass model is more luminous than the Popper's data. D'Antona & Mazzitelli (1985-14) noted that in all the recent computations the slope of the M-L relation sharply increase for masses smaller than $0.2M_{\odot}$. The exception of Grossman's models has not been understood by them. This exception also is satisfied for our population II models.

Following Chapter 1 and Section 2-1, low mass stars are difficult targets for both theoretical and observational studies. The agreement between theory and observation of these low luminous stars is still unsatisfactory. To the best of my knowledge, the best agreement between theory and observation, up to now, is for the models calculated by Grossman et al.(13). Although in their paper

below $0.15M_{\odot}$ there is not good agreement except at $0.085M_{\odot}$, Reid & Gilmore found a better fit to the Grossman's models of their observational data. The discrepancy between theory and observation could be the results of the uncertainties of both theoretical and observational data. In theoretical works, on the low mass models, the important source of the uncertainties are M dwarfs model atmosphere ($T(\tau)$ relation), thermodynamic functions, molecular opacities and all other parameters regarding the equation of state (see also 31,13,30). On the other hand all effects, mentioned in the last section, which contribute to the slope of the zero age line determine the accuracy of the models, contribute to the discordance of the two kinds of data. In general the M-L relations show better agreement with observation than the temperature-luminosity relations. This may be due to the $T(\tau)$ relation (see 13) and atmospheric opacities (see 6) which cause more uncertainty in effective temperature of M dwarfs. Near $0.2M_{\odot}$, models are fully convective and are sensitive to the mixing length and boundary conditions. Lowering α, as mentioned last section and concluded by Cox et al. (1981-30), may fit the models with the observed M-L relation. D'Antona (14) suggested even neglecting rotation as the

largest source of uncertainty and therefore deviation of their models from the observed mass-radius relation.

5- CONCLUSION

The slope of the zero age line in lower main sequence models is affected by the low temperature opacities and nonideal gas effects, as well as some other parameters including mixing length. This slope is different with that of the higher mass stars. The break occurs at a point of $\log T_e = 3.60\text{-}3.68$ depending on the composition and molecular opacities and equation of state. Ignoring molecular opacities shifts the position of the models in the H-R diagram toward the higher temperature and luminosities, but the simplified (exclusion of molecules) equation of state has the opposite effect of decreasing luminosity and effective temperature.

Decreasing mixing length parameter, α, also shifts the models toward the lower temperature and luminosity but this is not as effective as the molecules. The luminosity of the lowest mass models is more sensitive to the mixing length than massive ones. The best case for an evolutionary $1.0M_{\odot}$ model is inclusion of molecular equation of state with $\alpha=2.0$ which after $t=3.7E10^9$ to $t=3.8E10^9$ gives $R\approx 1.0R_{\odot}$ and $L\approx 1.0L_{\odot}$. Our final conclusion is that the

accuracy of the low mass models will be determined by the low temperature opacities and nonideal gas effects in the equation of state, as well as all other parameters regarding the properties of the low mass stars.

The slope of the zero age line is unaffected by composition change, but the location, on the H-R diagram, of the lower main sequence models will change with composition. At $0.3M_{\odot}$ a change from population I to population II shifts the model by $\Delta \log T_e = 0.067$ and $\Delta \log L/L_{\odot} = 0.227$. For a given temperature lower mass metal poor stars will be subluminous compared to the metal rich ones. A reduction in X (hydrogen abundant) results in an increase in the effective temperature and luminosity of the models. Models with $M \leq 0.2M_{\odot}$ of population II composition are fully convective.

Population I models are in good agreement with observational data of Reid & Gilmore(8) and Popper (33) in all the H-R, radius-luminosity, and mass-luminosity diagrams, although above the break (T_b) there is a discrepancy in effective temperature or radius. For population II (using $\alpha=1.0$) there are two deviations around $\log L/L_{\odot} = -1.4$ and -0.35. The higher and lowest mass models are in better agreement in the H-R diagram and radius-luminosity

Appendix I REFERENCES

1-H. Aller & Dean B. M., 1965. In "stellar structure" vol. VIII stars and stellar system, Chicago press.

2-T. R. Carson, 1969. In "Stellar evolution" Ed. Chiu & Muriel, 1972, The MIT press., p. 427.

3-Rosseland, 1924. Mon. Not. R. Astr. Soc., 84 , 525.

4-Limber, 1958. Astrophys. J., 127 , 387.

5-Kumar, 1962. Astrophys. J., 137 , 1121.

6-J. Liebert & Ronald G. P., 1987. Ann. Rev. Astr. Astrophys, 25 , 473.

7-M. S. Vardya, 1970. Ann. Rev. Astr. Astrophys., 8 , 87.

8-N. Reid & Gilmore, 1984. Mon. Not. R. Astr. Soc., 206 , 19.

9-G. Bertelli, A. Bressan, C. Chiosi & K. Angerer, 1986. Astron. Astrophys. Suppl. Ser., 66 , 191.

10-Schwarzschild, 1958. In "Structure and Evolution of the stars".

11-Mihalas, 1970. "Stellar Atmospheres", Freeman, San Francisco.

12-Chiu, 1968. In "Stellar physics", vol. 1, Blaisdell, Waltham.

13-A. S. Grossman, D. Hays, & H. C. Graboske, 1974. Astr. Astrophys. , 30 , 95.

14-Francesca D'Antona & I. Mazzitelli, 1985. Astr. J. , 296 , 502.

15-T. Van der Linden & R. Staller, 1982. Astron. Astrophys. 118 , 285.

16-Clayton, 1968. "Principles of Stellar Evolution and

Nucleosynthesis", McGraw-Hill, New York.

17-T. R. Carson, 1976. Ann. Rev. Astron. Astrophys., 14 , 95.

18-R. Kippenhahn, A. Weigert, and E. Hofmeister, 1967. In "Methods in Computational Physics", Vol. 7 Astr., Ed. Alder, Academic press, New York, p. 129.

19-I. Iben & A. Renzini , 1984. Phy. Rep. 105 , No. 6, p. 329.

20-R. F. Stein, 1966. In "Stellar Evolution" Ed. Stein & Cameron, Plenum press, p. 3.

21-H. Copeland , J. O. Jensen, and H. E. Jorgensen, 1970. Astron. Astrophys. 5 ,12.

22-G. D. Neece, 1984. Ast. J., 277 , 738.

23-I. Iben, 1967. Ann. Rev. Astr. Astrophys., 5 , 571.

24-T. J. Van der Linden, 1986. Astr. Astrophys. , 171 , 87.

25-S. A. Becker, 1981. Astrophys. J. Supp. Ser., 45 , 475.

26-J. G. Mengel, A. V. Sweigart, P. Demarque, and Gross, 1979. Astrophys. J. Supp. Ser., 40 , 733.

27-B. Paczynski, 1969. In "Stellar Evolution" Ed. Chiu& Muriel, 1972, The MIT press, p. 129.

28-C. Alcock & B. Paczynski, 1978. Ast. J., 223 , 244.

29-Fowler, Caughlin, and Zimmerman, 1975. Ann. Rev. Astr. Astrophys., 13 , 69.

30-D. A. Vandenberg, F. D. A. Hartwick, Dawson, and Alexander, 1983. Ast. J. 266 , 747.

31-R. Sienkiewicz, 1982. Acta. Astronomica 32 , No. 3-4, p. 275.

32-A. N. Cox, G. Shaviv, and S. W. Hodson, 1981. Ast. J. 245 , L37.

33-D. M. Popper, 1980. Ann. Rev. Astr. Astrophys. 18 , 115.

Appendix II

Physical and astrophysical constants used in the Thesis.

k	Boltzman's constant	1.381E-16 erg $^{o}K^{-1}$
m_H	hydrogen mass atom	1.672E-24 g
G	gravitational constant	6.670E-8 dyn cm^2 g^{-2}
a	radiation constant	7.5648E-15 erg cm^{-3} deg^{-4}
c	velocity of light	2.998E10 cm sec^{-1}
h	Planck's constant	6.62619E-27 erg sec
e	electron charge	1.602E-20 emu
M_Θ	solar mass	1.989E33 g
L_Θ	solar luminosity	3.826E33 erg sec^{-1}
R_Θ	solar radius	6.9598E10 cm
σ	Stefan-Boltzman constant	5.6696E-5 erg cm^{-2} sec^{-1} $^{0}K^{-4}$
σ_T	Thomson cross section	6.65245E-25 cm^2
R	gas constant	8.3143E7 erg $^{o}K^{-1}$ $mole^{-1}$
r_0	classical electron radius	2.817939E-13 cm